SAFE-LAND

Mitigating the risk of flooding and landslides via artificial intelligence with a view to extreme climate events

Deliverable 3.2:
Hydrogeological risk assessment of reference areas

MITIGATING THE RISK OF FLOODING AND LANDSLIDES VIA ARTIFICIAL INTELLIGENCE WITH A VIEW TO EXTREME CLIMATE EVENTS

Co-funded by the European Union

eCAMPUS UNIVERSITÀ
UNIVERSITÀ DI PISA
MEĐIMURSKA ŽUPANIJA

Deliverable Title	Hydrogeological risk assessment of reference areas
Deliverable number	3.2
Deliverable Lead:	eCampus
Related Work Package:	WP3: Hydrogeological risk assessment, evaluation of people's risk awareness, and guidelines for reference areas
Author(s):	Elisabetta Cattoni (eCampus), Stefano Pagliara (UNIPI), Elena Camisasca (eCampus), Fabrizio Comodini (eCampus), Alberto Dusi (eCampus), Francesco Focacci (eCampus), Ignacio Giomi (eCampus), Michele Palermo (UNIPI), Cristal Sirotich (eCampus), Salvatore Verre (eCampus), Evelina Volpe (eCampus).
Dissemination Level:	Public
Due Submission Date:	11/06/25
Actual Submission:	16/07/25
Project Number	101140345
Status	Version 2.0 (16/07/25)
Reviewed (Authors)	Francesco Pistolesi (UNIPI), Zorica Marković (MUP), Marija Marciuš (MED)
Start Date of Project:	12 February 2024
Duration:	24 months
Abstract	This document is the Deliverable 3.2 of the project "M*itigating the risk of flooding and landslides via artificial intelligence with a view to extreme climate events* (SAFE-LAND)". The deliverable describes the procedures and the analyses performed to assess the landslide and flood risk of reference elements (respectively slopes and rivers) subjected to the reference climate events, and the evaluation of risk awareness of the reference elements (people). The results of these analyses provide the knowledge base (KB) used to train the Trustworthy Artificial Intelligence system.
Status changes history	Version 1.0 (11/06/2025) – First release Version 2.0 (16/07/25)– Second release

Funded by the European Union. Views and opinions expressed are however those of the author(s) only and do not necessarily reflect those of the European Union. Neither the European Union nor the granting authority can be held responsible for them.

TABLE OF CONTENTS

Funded by the European Union. Views and opinions expressed are however those of the author(s) only and do not necessarily reflect those of the European Union. Neither the European Union nor the granting authority can be held responsible for them.

1. INTRODUCTION

The landslide and flooding risk level of each *reference* element subjected to a *reference* climate event is evaluated by performing analytical/numerical analyses based on hydrogeological data (slope and river elements), and psychological data (people element).
These reference elements, which constitute the basis of the knowledge-based (KB) dataset, are not real cases but are purposely designed to train the AI system. Different values of element parameters (EPs) were considered to cover the widest range of possible existing cases to set up the KB dataset, which is being used to train the AI tool.
The results of the numerical analyses provide the damage parameters (DPs) which allow to measure the risk of each reference element subjected to the reference climate events (RCEs). The DPs values and the EPs values of all reference elements constitute the KB dataset (*training data*) and are used to train the AI system. Therefore, when the AI system will be applied in a real area using the data of a real element (*testing data*), it will be able to evaluate the DPs values of the real element, based on similarity criteria.

This document describes the procedures and the numerical analyses performed to evaluate the damage parameters values for each reference element, to assess the risk of landslide and flooding, and the risk awareness.
The document is organized as follows. Section 2 and 3 provide the description of the numerical analyses and procedures followed to evaluate the landslide and flood risk of the reference slopes and rivers respectively. In Section 4 the description of the risk awareness of reference people is reported.

2. LANDSLIDE RISK ASSESSMENT OF REFERENCE ELEMENTS (SLOPES)

Landslide risk can be quantified based on the following key components: hazard and consequences; the latter can be considered as the product of vulnerability and exposed elements. Mathematically, risk R is expressed as:

$$R = H \cdot C = H \cdot V \cdot E$$

where:

H represents the hazard, defined as the probability of occurrence of a landslide;
C denotes the consequences, which encompass both vulnerability assessment and exposure analysis of at-risk elements;
V is the vulnerability, referring to the degree of potential loss that an exposed element may sustain when subjected to the given hazard;
E indicates the elements at risk, encompassing assets, infrastructure, populations, or

Co-funded by the European Union

Funded by the European Union. Views and opinions expressed are however those of the author(s) only and do not necessarily reflect those of the European Union. Neither the European Union nor the granting authority can be held responsible for them.

environmental components susceptible to damage.

A risk analysis process includes the hazard analysis phase - considering the potential landslide and the probability of occurrence – and the consequence analysis - quantifying the elements at risk (properties and people), and their vulnerability either as probability of damage to property, or probability of loss of life on injury (Fell et al., 2005).

The following Sections 2.1 and 2.2 describe the procedures followed to:
- perform the landslide hazard assessment of the reference slopes
- establish the criteria to evaluate the landslide risk of a given area.

2.1. HAZARD ASSESSMENT

2.1.1. Slopes stability analyses

The TAI system uses damage parameters of the reference slope elements in order to:
- evaluate the landslide risk, using mainly the slope's factor of safety (*FoS*) as damage parameter;
- suggest the most suitable mitigation measures in the case of $FoS \leq 1$, using as additional damage parameters the depth of the sliding surface (z_s), and the depth of the piezometric level at the end of the infiltration process induced by a rainfall (z_w^{final}).

Damage parameters are determined via numerical analyses performed with GeoStudio codes, SEEP/W and SLOPE/W (Geostudio, 2024).
The numerical analyses for reference slopes were carried out considering the effect of different reference climatic events (rainfalls), characterized by various return periods and accumulated precipitation. In particular, infiltration analyses induced on a given slope by a given rainfall were carried out using SEEP/Wcode, and slope stability analyses with SLOPE/W code, by incorporating the hydraulic conditions altered by the input rainfall.
A comprehensive 2D numerical dataset was generated, where several combinations of geometrical, mechanical and hydraulic parameters were considered, also combined with different rainfalls and initial water table locations. With the hydro-mechanical model implemented in Geostudio codes, about 23,500 simulations were carried out to identify the landslide hazard associated with reference rainfall events, and to predict the triggering of instabilities in slope. This dataset will be used to train the TAI system aimed at assessing slope stability across varying environmental scenarios.

Co-funded by the European Union
Funded by the European Union. Views and opinions expressed are however those of the author(s) only and do not necessarily reflect those of the European Union. Neither the European Union nor the granting authority can be held responsible for them.

Modeling the slope element in SLOPE/W

The mechanical model was analyzed using a 2D approach in SLOPE/W, which enables slope stability assessments through various limit equilibrium methods, e.g., Fellenius, (1936), Janbu, (1954), Bishop (1955), Morgenstern-Price (1965), Spencer (1967). These methods evaluate slope stability by examining the relationship between the ultimate shear strength and mobilized shear stresses. For the reference slopes in the dataset, the Morgenstern-Price (1965) method was selected. The differences between the cited approaches lie in the statistical equations used and the treatment of interlaced forces to define shear and normal forces. The Morgenstern-Price (1965) method incorporates iterative processes, considers both normal and shear interlaced forces, and satisfies equilibrium and momentum statics equations.
The general limit equilibrium (GLE) formulation integrated into SLOPE/W and used in the analyses to define the factor of safety (*FoS*), follows the interlaced force function for the Morgenstern-Price method:

$$X = E\lambda f(x)$$

where, *f(x)* is an arbitrary function that defines the variation of the force X with respect to E, λ a scaling factor, *E* the interlace normal force, and X the interlace shear force. Different forms regarding the function f(x) can be chosen, e.g., constant, half-sine, clipped-since, trapezoidal and data-point, having little influence on the final result, but it is important to verify that the obtained values are physically acceptable. For its applicability, the half-sine slide function was selected.
The critical slip surface, associated with the lowest factor of safety, can be defined using various methods, including the grid and radius approach for circular slips, fully specified surfaces, exit and entry values, block-specified slip surfaces, specific parallel forms, and optimization techniques. For the reference slope models, the exit and entry specification (Fig. 2.1) was selected, allowing precise definition of the most likely trial slip surface's entry and exit points on the ground surface. To ensure consistency across simulations, the entry and exit points were positioned at ground level, adjacent to the slope, extending across the entire soil domain, as illustrated in Fig. 2.1.

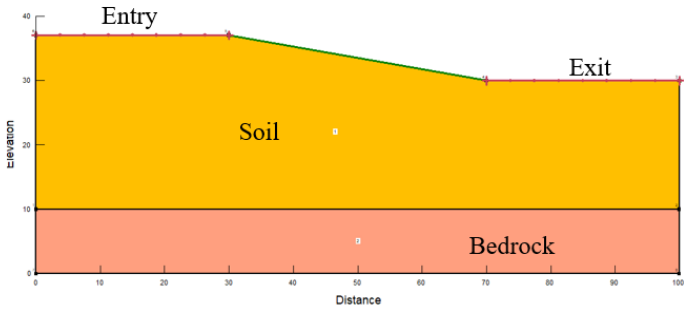

Figure 2.1: Specification of the entry and exit.

Funded by the European Union. Views and opinions expressed are however those of the author(s) only and do not necessarily reflect those of the European Union. Neither the European Union nor the granting authority can be held responsible for them.

The strength of the material (soil) was described by the Mohr-Coulomb model. The shear strength is expressed by the following equation:

$$\tau = c' + \sigma'_n tan\,(\varphi')$$

where, c' is the effective cohesion, φ' is the effective friction angle, and σ'_n is the effective normal stress in the shear plane. In SLOPE/W, the bedrock (the lowest layer of the domain, as shown in Fig. 2.1) can be defined as an impenetrable surface, and considered a non-flux boundary.

The domain of the soil upper the piezometric level was considered as unsaturated. The shear strength under this condition can be rewritten by the following approach (Vanapalli et al., 1996):

$$\tau = c' + (\sigma'_n - u_a)tan\,(\varphi') + (u_w - u_a)\left[\left(\frac{\theta_w - \theta_r}{\theta_s - \theta_r}\right)tan\,(\varphi')\right]$$

where u_w is the pore water pressure, u_a is the pore-air pressure, θ_ω is the volumetric water content, θ_r is the residual water content and θ_s is the saturated water content. The location of the water table level along with the volumetric water content considered in Geoslope analysis was taken from the results of SEEP/W analysis.

The specified unit weight is taken into account in the total weight of the slice. The total weight must be specified as total unit weight since SLOPE is formulated based on total forces. Above the water table, the soil is considered unsaturated (the unit weight will depend on the degree of saturation) and below the water table as saturated. The total unit weight is given by:

$$\gamma = \gamma_w\left(\frac{G_s + Se}{1 + e}\right)$$

where, γ_w is the water unit weight, G_s the specific gravity, S the degree of saturation and e the void ratio.

Sensitivity analysis

The variables were selected by following a Gaussian Probability Distribution whose density function that can be express as follow:

$$f(x) = \frac{e^{-(x-u)^2/2\sigma^2}}{\sigma\sqrt{2\pi}}$$

where x is the variable of interest, u the mean value and σ the standard deviation. The selected parameters/variables were the effective cohesion, the effective angle of internal friction and

Funded by the European Union. Views and opinions expressed are however those of the author(s) only and do not necessarily reflect those of the European Union. Neither the European Union nor the granting authority can be held responsible for them.

the unit weight. In the sensitivity analyses performed in SLOPE/W, one variable is varied while the others are kept constant. This shows how each variable affects the output of the stability model. For each combination of parameters, the program returns the lowest *FoS*, associated with the critical slip surface.

Modeling the slope element in SEEP/W

For each considered geometry of the slope, the hydraulic models to represent the behavior of the slope under different scenarios of rainfall and different hydraulic parameters were analyzed.

SEEP/W uses the finite element method to analyze the flow of water through saturated and unsaturated porous media. For the proposed models, a transient analysis was performed based on the changes in precipitation intensity over time, to determine how these changes can modify the volumetric water content in the soil domain and can cause changes in the water table level. For the soil domain, a saturated-unsaturated model was considered. Thus, above the water table, the properties are governed by the unsaturated condition, while, under the water table, the soil is completely saturated. For simplicity, no anisotropy was considered in the hydraulic properties. To analyze the variation of the hydraulic behavior, three different profiles of soil were considered: a sand, a clay and a silt. The values of the retention curve are based on the predefined profiles implemented in SEEP/W to represent typical values of this different soil based on experimental data reported in the literature. The volumetric water content according to van Genuchten (1980) can be expressed by the following equation:

$$\theta_w = \theta_{res} + \frac{\theta_{sat} - \theta_{res}}{[1 + (a's)^n]^m}$$

where a', n and m are the fitting parameters of the van Genuchten (1980) equation, ϑ_{res} is the residual volumetric water content and θ_{sat} the saturated water content.

2.1.2. Reference slopes, simulations program, and results in terms of DPs

Parameters defining the reference slopes can be categorized into geometric parameters, and mechanical and hydraulic soil parameters. Figures 2.2 provide schematic representations of the geometry of a generical reference slope. The analyses combined geometrical, mechanical, and hydraulic parameters defined across specific ranges to assess slope stability based on the factor of safety for different soil types. The considered geometrical variables were the slope angle (α),

Funded by the European Union. Views and opinions expressed are however those of the author(s) only and do not necessarily reflect those of the European Union. Neither the European Union nor the granting authority can be held responsible for them.

slope length (L), total length (B), slope height (H), total height - upstream (h_u), total height - downstream (h_d), soil depth - upstream (h_{Su}), soil depth - downstream (h_{Sd}), bedrock depth - upstream (h_{Bu}) and bedrock depth – downstream (h_{Bd}). The positions of the water tables were defined upstream (z_{wu}) and downstream (z_{wd}), before (z_{wu}^{init} - z_{wd}^{init}) and after (z_{wu}^{final} - z_{wd}^{final}) the precipitation.

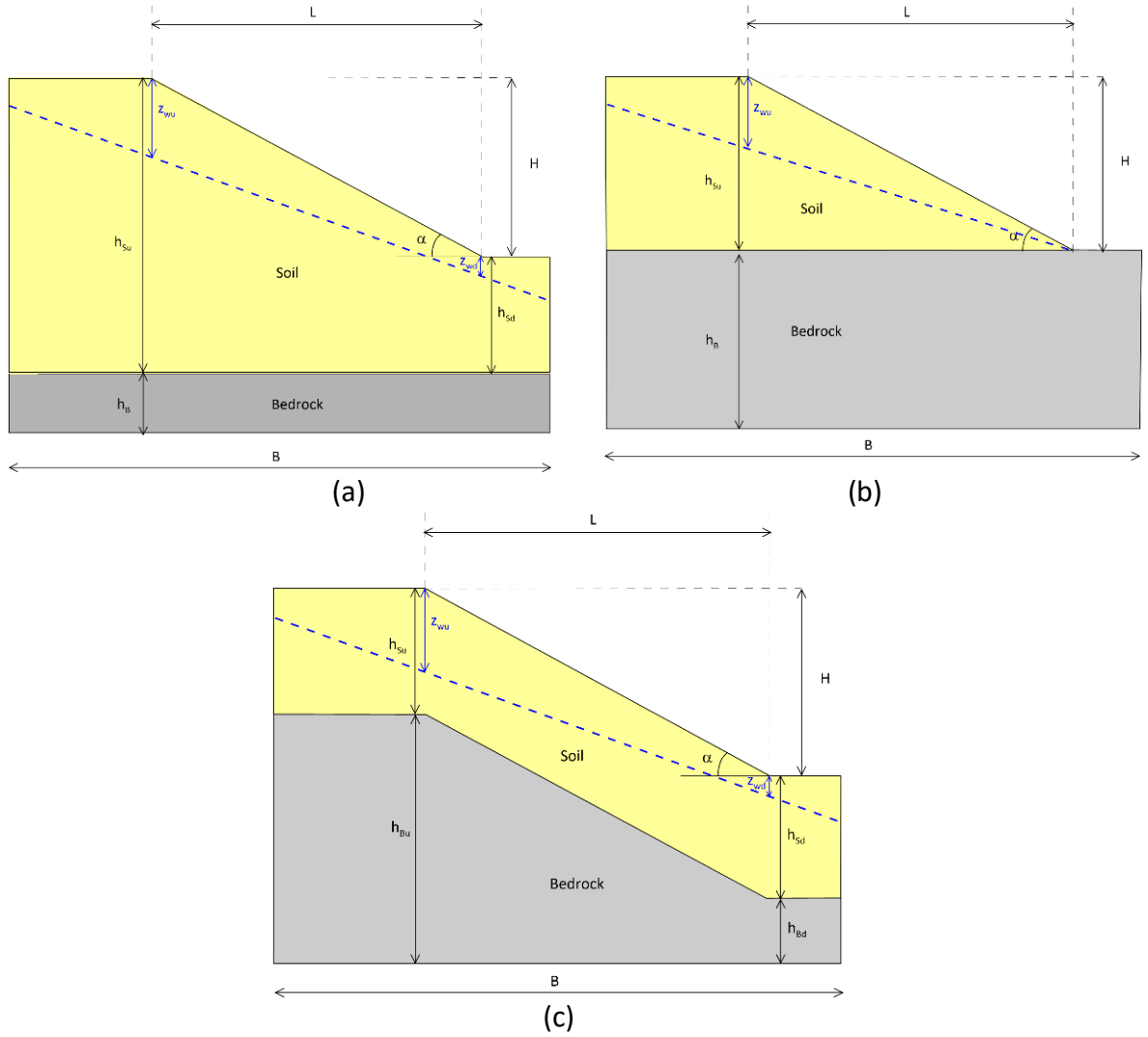

Figure 2.2: Slope geometries: (a-b) horizontal bedrock; (c) inclined bedrock.

Funded by the European Union. Views and opinions expressed are however those of the author(s) only and do not necessarily reflect those of the European Union. Neither the European Union nor the granting authority can be held responsible for them.

Simulations program

Sensitivity analyses were performed in SLOPE/W, while one the variables change, the others are kept constant, in order to evaluate the effect of each variable on the *FoS* value.

Three different scenarios were considered to analyze the response of the slope element, two of them in drained conditions (D.1 and D.2) and the third one, in undrained conditions (UN).

Tables 2.1 summarize the parameter values adopted for the geometrical combinations. For D.1 analyses, four ratios between the soil strata and the bedrock were evaluated. The first two ratios considered a horizontal bedrock with $h_{Su(90)}$ =0.9 h_u and $h_{Sd(90)}$ = $h_{Su(90)} - H$ (Fig. 2.2a), and $h_{Su(H)}$ = H and $h_{Sd(H)}$ = 0 (Fig. 2.2b). The third and the fourth cases considered an inclined bedrock, where $h_{Su(25)}$ = 0.25 h_u, and $h_{Sd(25)}$ = 0.25 h_d, and $h_{Su(2)}$ = 2 m and $h_{Sd(2)}$ = 2m (Fig. 2.2c).

In the case of undrained conditions (UN) the same parameters as those in Table 2.1a were considered, but the sensitivity analyses were not performed on the $h_{Su(2)}$ = 2 m and $h_{Sd(2)}$ = 2m.

For D.2 analyses, a horizontal bedrock was assumed (Fig 2.2a), where three different values of the soil depth - upstream (h_{Su}), and - downstream (h_{Sd}) were assumed (Table 2.2b).

Table 2.1. Geometrical parameters: (a) drained (D.1) and undrained conditions (UN); (b) drained conditions (D.2)

(a)

α (°)	L (m)	B (m)	H (m)	h_u (m)	h_d (m)	h_{Su} (m)				h_{Sd} (m)			
						$h_{Su(90)}$	$h_{Su(25)}$	$h_{Su(H)}$	$h_{Su(2)}$	$h_{Sd(90)}$	$h_{Sd(25)}$	$h_{Sd(H)}$	$h_{Sd(2)}$
20	20	100	7.3	25	17.7	22.5	6.3	7.3	2.0	15.2	4.4	0.0	2.0
	40	200	14.6	45	30.4	40.5	11.3	14.6	2.0	25.9	7.6	0.0	2.0
	80	400	29.1	90	60.9	81.0	22.5	29.1	2.0	51.9	15.2	0.0	2.0
30	20	100	11.5	35	23.5	31.5	8.8	11.5	2.0	20.0	5.9	0.0	2.0
	40	200	23.1	70	46.9	63.0	17.5	23.1	2.0	39.9	11.7	0.0	2.0
	80	400	46.2	140	93.8	126.0	35.0	46.2	2.0	79.8	23.5	0.0	2.0
40	20	100	16.8	50	33.2	45.0	12.5	16.8	2.0	28.2	8.3	0.0	2.0
	40	200	33.6	100	66.4	90.0	25.0	33.6	2.0	56.4	16.6	0.0	2.0
	80	400	67.1	200	132.9	180.0	50.0	67.1	2.0	112.9	33.2	0.0	2.0
50	20	100	23.8	70	46.2	63.0	17.5	23.8	2.0	39.2	11.5	0.0	2.0
	40	200	47.7	145	97.3	130.5	36.3	47.7	2.0	82.8	24.3	0.0	2.0
	80	400	95.3	290	194.7	261.0	72.5	95.3	2.0	165.7	48.7	0.0	2.0

Funded by the European Union. Views and opinions expressed are however those of the author(s) only and do not necessarily reflect those of the European Union. Neither the European Union nor the granting authority can be held responsible for them.

(b)

α (°)	*L* (m)	*B* (m)	*H* (m)	h_{Bu} (m)	h_{Bd} (m)	h_{Su} (m)			h_{Sd} (m)		
						h_{Su1} (m)	h_{Su2} (m)	h_{Su3} (m)	h_{Sd1} (m)	h_{Sd2} (m)	h_{Sd3} (m)
30	40	100	23.1	10.0	10.0	35.0	45.0	55.0	11.9	21.9	31.9
	80	160	46.2	10.0	10.0	60.0	70.0	-	13.8	23.8	-
40	20	60	16.8	10	10.0	25.0	30.0	35.0	8.2	13.2	18.2
45	20	60	20.0	10	10.0	30.0	35.0	40.0	10.0	15.0	20.0

The mechanical parameters varied under drained conditions (D.1 and D.2) were the effective cohesion (c'), effective friction angle (ϕ'), and soil unit weight (γ), while under undrained conditions (UN), the undrained cohesion (c_u) and the soil unit weight (γ) were considered. Table 2.2 shows the adopted mean values (μ), range of variation, and increment (Δ) for each case. The ranges adopted for drained conditions are representative of sandy, silty and clayey soils; for the undrained condition, the adopted values are typical for clayey soils (Mitchell and Soga 2005; Budhu, 2015).

Table 2.2. Mechanical parameters in drained (D.1 and D.2) and undrained (UN) conditions

Condition	Mechanical properties	μ	Range	Δ
D.1	Effective cohesion, c' (kPa)	20	0-40	10
	Effective Friction Angle, φ' (°)	25	5-45	10
	Soil Unit Weight γ (kN/m^3)	18	12-24	3
D.2	Effective cohesion, c' (kPa)	20	0-40	5
	Effective Friction Angle, φ' (°)	25	0-50	5
	Soil Unit Weight γ (kN/m^3)	15	9-21	2
UN	Undrained cohesion, c_u (kPa)	175	25-325	50
	Soil Unit Weight γ (kN/m^3)	18	12-24	3

Table 2.3 presents the hydraulic parameter sets reflecting variability in the hydraulic behavior of three types of soil. Soil type 1 is characterized by high saturated hydraulic conductivity, typically representative of sandy soils. Soil type 2 has an intermediate value, as observed in silty soils. Soil type 3 corresponds to a low value of hydraulic conductivity, representative of clayey soils. Different values of saturated conductivities for D.1 and D.2 were considered to cover the full range of possible permeabilities. The analyses D1 and D2 were performed for each type of soil (1, 2, and 3), while the analyses UN were performed only for soil type 3 with low permeability, due the drained behavior of the other types of soil also in short-time conditions.

Fitting parameters that describe the unsaturated behavior, based on the van Genuchten (1980)

Funded by the European Union. Views and opinions expressed are however those of the author(s) only and do not necessarily reflect those of the European Union. Neither the European Union nor the granting authority can be held responsible for them.

equation, are also included in Table 2.3. The range of suction was specified according to the expected range for each soil (sand, silt and clay) as an upper bound. Fig. 2.3 presents the SWRC curves and the fitting parameters adopted, available in the Geoslope library (Geostudio, 2024). For the bedrock it was assumed a fully saturated condition, with a very low hydraulic conductivity (1e-12 m/s), without flow through this layer.

Table 2.3. Hydraulic parameters

Condition	Soil type	K_{sat} (m/s)	van Genuchten (1980)		
			α (kPa-1)	*n*	*m*
D.1	1	1.00E-04	0.5	2	0.500
	2	1.00E-06	0.08	1.7	0.412
	3	1.00E-08	0.02	1.5	0.333
D.2	1	1.00E-03	0.5	2	0.500
	2	1.00E-05	0.08	1.7	0.412
	3	1.00E-07	0.02	1.5	0.333
UN	3	1.00E-08	0.02	1.5	0.333

Rainfall was modeled by applying surface water fluxes ($mm^3/h/mm^2$) at the ground level, simulating low, medium, and high rainfall intensities, corresponding to 30-, 200-, and 500-year return periods, respectively. The precipitation was distributed using Chicago hyetographs with a central peak (Fig. 2.4).

Table 2.4 contains the characteristics of the rainfall events in terms of return period (T_r), duration (d), and accumulated precipitation (h_w). For the D.1 and UN conditions, the *FoS* was obtained for the base scenario (without precipitation) and at the end of a 100-hour event; for the D.2 condition, the response was evaluated at different time steps (0, 15, and 30 hours).

Funded by the European Union. Views and opinions expressed are however those of the author(s) only and do not necessarily reflect those of the European Union. Neither the European Union nor the granting authority can be held responsible for them.

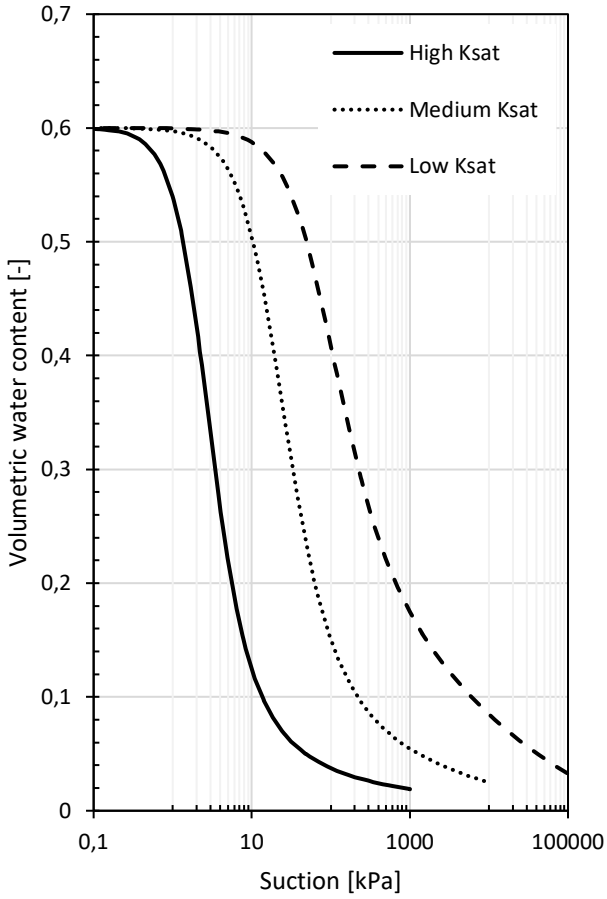

Figure 2.3: Soil water retention curves for the modeled soils.

Three groundwater table scenarios were considered: (1) high water table (z_{w1}^{init}), matching the ground surface; (2) low water table (z_{w2}^{init}), aligned with the bedrock surface; (3) intermediate water table (z_{w3}^{init}), located between the ground surface and the bedrock.

Table 2. 4. Rainfall events

Condition	Intensity, *i*	Return Period, T_r (years)	Duration, *d* (hours)	Accumulated precipitation, h_w (mm)
D.1 - UN	Low	30	100	315.90
	Medium	200	100	480.50
	High	500	100	586.00
D.2	Low	30	30	200.29
	Medium	200	30	305.90
	High	500	30	371.45

Co-funded by the European Union
Funded by the European Union. Views and opinions expressed are however those of the author(s) only and do not necessarily reflect those of the European Union. Neither the European Union nor the granting authority can be held responsible for them.

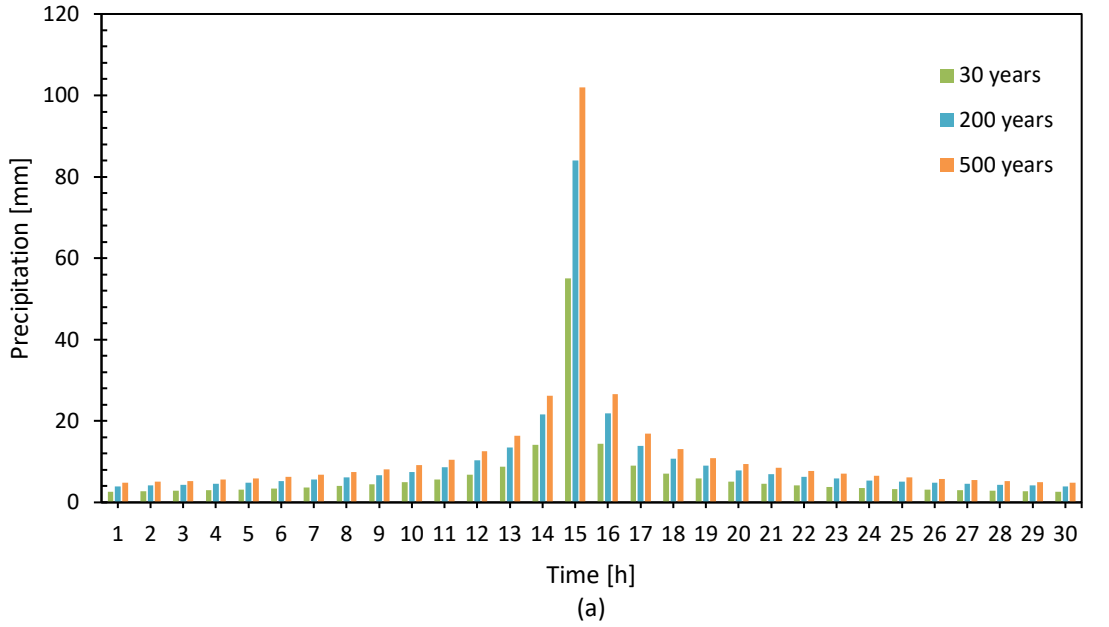

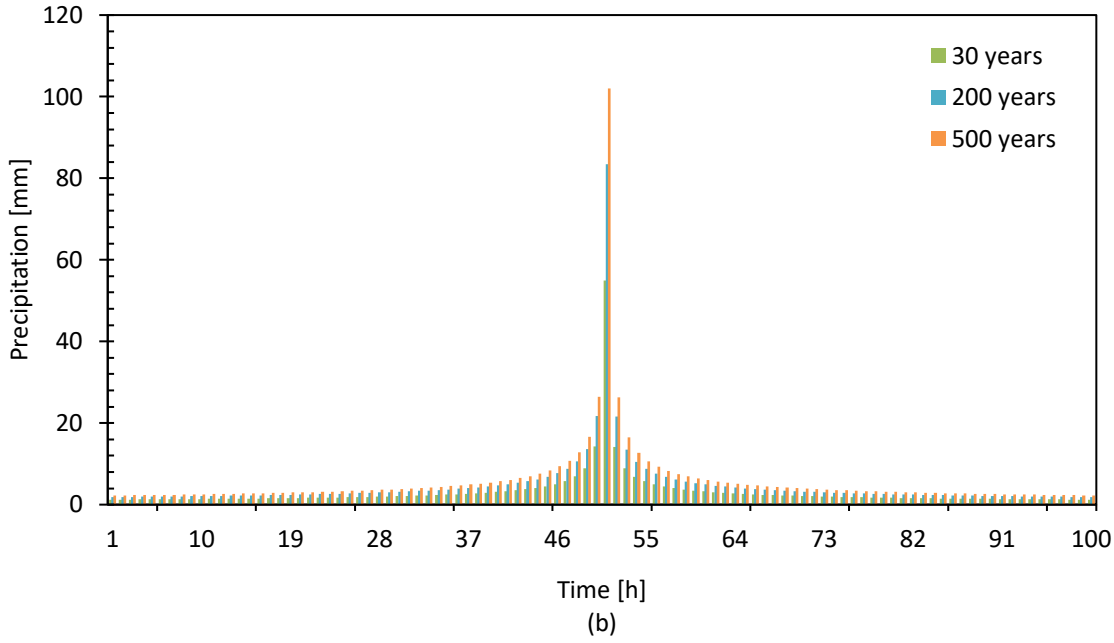

Figure 2.4: Precipitation events adopted for the simulations.

Co-funded by the European Union

Funded by the European Union. Views and opinions expressed are however those of the author(s) only and do not necessarily reflect those of the European Union. Neither the European Union nor the granting authority can be held responsible for them.

The dataset consists of about 23,500 simulations:

1) Drained condition (D.1): 48 combinations of geometrical parameters (Table 2.1a), 3 types of soil based on hydraulic characteristics ($K_{sat,1}$, $K_{sat,2}$, and $K_{sat,3}$), as reported in Table 2.3, 3 rainfall events (i_1, i_2, and i_3), and a base scenario i0 without precipitation (Table 2.4), 3 initial positions of the water table (z_{w1}^{init}, z_{w2}^{init}, and z_{w3}^{init}), and 13 combinations of mechanical parameters (Table 2.2). Table 2.5 summarizes the combinations of parameters for each row of Table 2.1a. In total, 13,572 simulations were carried out to explore all possible combinations in D.1.
2) Drained condition (D.2): 11 combinations of geometrical parameters (Table 2.1b), 3 types of soil based on hydraulic characteristics ($K_{sat,1}$, $K_{sat,2}$, and $K_{sat,3}$), 3 rainfall events (i_1, i_2, and i_3), at two different times steps (15 and 30 hours), and the base scenario i0, 1 initial position of the water table (z_{w3}^{init}), and 25 combinations of mechanical parameters (Table 2.2). Table 2.6 summarizes the simulated cases for each combination of geometrical parameters (5,775).
3) Undrained conditions (UN): 36 combinations of geometrical parameters (Table 2.1a), 1 hydraulic conductivity ($K_{sat,3}$), the same precipitation events and phreatic positions as D.1, and 11 combinations of mechanical parameters. Table 2.7 summarizes the simulation analyses performed (total amount 4,212).

In Tables 2.5 and 2.7, the number of simulations for the first phreatic level (z_{w1}^{init}) is lower than those of the other positions (z_{w2}^{init} and z_{w3}^{init}), as the effect of the rainfall was neglected due to the pre-existing complete saturation of the soil.

Funded by the European Union. Views and opinions expressed are however those of the author(s) only and do not necessarily reflect those of the European Union. Neither the European Union nor the granting authority can be held responsible for them.

Table 2.5 Simulations performed in drained conditions (D.1)

Geometry	h_{su}	z_w^{init}	K_{sat}	*Intensity, i*	Simulation ID
α, L, B,H, h_u	$h_{Su(90)}$	z_{w1}^{init}	$K_{sat,1}$	i_0	1-13
			$K_{sat,2}$		
			$K_{sat,3}$		
		z_{w2}^{init}	$K_{sat,1}$	i_0, i_1, i_2, i_3	14-65
			$K_{sat,2}$	i_0, i_1, i_2, i_3	65-117
			$K_{sat,3}$	i_0, i_1, i_2, i_3	118-169
		z_{w3}^{init}	$K_{sat,1}$	i_0, i_1, i_2, i_3	170-221
			$K_{sat,2}$	i_0, i_1, i_2, i_3	222-273
			$K_{sat,3}$	i_0, i_1, i_2, i_3	274-325
	$h_{Su(25)}$	z_{w1}^{init}	$K_{sat,1}$	i_0	326-338
			$K_{sat,2}$		
			$K_{sat,3}$		
		z_{w2}^{init}	$K_{sat,1}$	i_0, i_1, i_2, i_3	339-390
			$K_{sat,2}$	i_0, i_1, i_2, i_3	391-442
			$K_{sat,3}$	i_0, i_1, i_2, i_3	443-494
		z_{w3}^{init}	$K_{sat,1}$	i_0, i_1, i_2, i_3	495-546
			$K_{sat,2}$	i_0, i_1, i_2, i_3	547-598
			$K_{sat,3}$	i_0, i_1, i_2, i_3	599-650
	$h_{Su(H)}$	z_{w1}^{init}	$K_{sat,1}$	i_0	651-663
			$K_{sat,2}$		
			$K_{sat,3}$		
		z_{w2}^{init}	$K_{sat,1}$	i_0, i_1, i_2, i_3	664-715
			$K_{sat,2}$	i_0, i_1, i_2, i_3	716-767
			$K_{sat,3}$	i_0, i_1, i_2, i_3	768-819
		z_{w3}^{init}	$K_{sat,1}$	i_0, i_1, i_2, i_3	820-871
			$K_{sat,2}$	i_0, i_1, i_2, i_3	872-923
			$K_{sat,3}$	i_0, i_1, i_2, i_3	924-975
	$h_{Su(2)}$	z_{w2}^{init}	$K_{sat,1}$	i_0, i_1, i_2, i_3	976-1027
			$K_{sat,2}$	i_0, i_1, i_2, i_3	1028-1079
			$K_{sat,3}$	i_0, i_1, i_2, i_3	1080-1131

Funded by the European Union. Views and opinions expressed are however those of the author(s) only and do not necessarily reflect those of the European Union. Neither the European Union nor the granting authority can be held responsible for them.

Table 2.6: Simulations for drained condition (D.2)

Geometry	h_{su}	z_w^{init}	K_{sat}	*Intensity, i*	Simulation ID
α, L, B,H	h_{Sui}	z_{w3}^{init}	$K_{sat,1}$	i_0, i_1, i_2, i_3	1-175
			$K_{sat,2}$	i_0, i_1, i_2, i_3	176-350
			$K_{sat,3}$	i_0, i_1, i_2, i_3	351-525

Table 2.7: Simulations for undrained condition (UN)

Geometry	h_{su}	z_w^{init}	K_s	*Intensity, i*	Simulation ID
α, L, B,H, h_u	$h_{Su(90)}$	z_{w1}^{init}	$K_{sat,3}$	i_0	1-13
		z_{w2}^{init}		i_0, i_1, i_2, i_3	14-65
		z_{w3}^{init}		i_0, i_1, i_2, i_3	66-117
	$h_{Su(25)}$	z_{w1}^{init}	$K_{sat,3}$	i_0	118-130
		z_{w2}^{init}		i_0, i_1, i_2, i_3	131-182
		z_{w3}^{init}		i_0, i_1, i_2, i_3	183-234
	$h_{Su(H)}$	z_{w1}^{init}	$K_{sat,3}$	i_0	235-247
		z_{w2}^{init}		i_0, i_1, i_2, i_3	248-299
		z_{w3}^{init}		i_0, i_1, i_2, i_3	300-351

For each analysis, slope stability was evaluated under saturated and unsaturated conditions, with a transient analysis by solving the water mass balance equation with the finite element method (FEM) in SEEP/W, followed by limit equilibrium analysis in SLOPE/W.
The outputs used as damage parameters (DPs) of each simulation were the factor of safety (*FoS*), the depth of the slip surface (z_s), and the final position of the water table after the precipitation event (z_w^{final}). The *FoS* leads to the risk assessment (slope unstable if $FoS \leq 1$), whereas z_s and z_w^{final} allow to indicate the most effective stabilization measures.

Table 2.8 shows the number of parameters adopted for each simulation phase performed for drained (D.1 and D.2) and undrained (UN) conditions, along with the total number of parameters obtained in output (*FoS*, z_s , z_w^{final}). The overall number of the hydro-mechanical slope stability analyses was 23,559.

Funded by the European Union. Views and opinions expressed are however those of the author(s) only and do not necessarily reflect those of the European Union. Neither the European Union nor the granting authority can be held responsible for them.

Table 2.8: Summary of parameters and analyses in GeoStudio.

Analyses	Parameters	Number of parameters			Number of OUTPUTS (FoS, z_s , z_w^{final})		
		D.1	D.2	UN	D.1	D.2	UN
SEEP/W	Hydraulic conductivity	3	3	1	13572	5775	4212
	Initial position of the phreatic level	3	1	3			
	Precipitations events	3	3	3			
	Soil-bedrock ratio	4	1	3			
SLOPE/W	Times steps	2	3	2			
	Mechanical parameters	13	25	11			

In the following an example numerical analyses is shown.
Table 2.9 presents the characteristics and results of a drained analysis (D.1) performed for a slope with an inclination of 40°, a slope length of 40 m and a total height upstream of 100 m. The geometrical, mechanical and hydraulic parameters are called *P* domain, and the response of the model compares the base scenario without precipitation (i_0) to the case of a 30-year return period precipitation event (i_1). The characteristics of the precipitation events are summarized as E domain. The domain C_p shows that the slope was stable (*FoS* = 1.118) before the precipitation (Fig. 2.7a), and after a 100-hour rainfall event, the slope became unstable (*FoS* = 0.938), as shown in Fig.2.7b. No big difference of the depth of the slips surface were observed, but the water table upstream raised from 22.4 m to 17.9 m from the ground level, reducing the shear strength of the soil and causing instability. Data from all domains will be used to train the AI system.

Co-funded by the European Union
Funded by the European Union. Views and opinions expressed are however those of the author(s) only and do not necessarily reflect those of the European Union. Neither the European Union nor the granting authority can be held responsible for them.

Table 2.9: Parameters adopted for the same precipitation event.

Domain	Parameters	Symbol	D.1	
			i_0	i_1
P	Unit weight (kN/m^3)	γ	18	18
	Effective cohesion (kPa)	c'	20	20
	Effective friction angle (°)	φ'	25	25
	Undrained Shear Strength (kPa)	C_u	-	-
	Saturated permeability (m/s)	k_{sat}	1E-04	1E-04
	Soil Type (-)	ST	1	1
	Slope angle (°)	α	40	40
	Slope length (m)	L	40	40
	Total length (m)	B	200	200
	Slope height (m)	H	34	34
	Total height Upstream (m)	h_m	100	100
	Total height Downstream (m)	h_d	66	66
	Soil depth upstream (m)	h_{Su}	90	90
	Soil depth downstream (m)	h_{Sd}	56	56
	Bedrock depth upstream (m)	h_{Bu}	10	10
	Bedrock depth downstream (m)	$h3_d$	10	10
	Initial piezometric depth - Upstream (m)	z_{wu}^{init}	22	22
	Initial piezometric depth -Downstream (m)	z_{wd}^{init}	0	0
E	Return period of precipitation (years)	T_r		30
	Accumulated precipitation (mm)	h_w	0	316
	Precipitation duration (hrs)	t_w	100	100
C_p	Factor of safety (-)	FoS	1.118	0.938
	Depth of slip surface (m)	z_s	16.0	17.0
	Final Piezometric depth - Upstream (m)	z_{wu}^{final}	22.4	17.9
	Final Piezometric depth -Downstream (m)	z_{wd}^{final}	0	0

Funded by the European Union. Views and opinions expressed are however those of the author(s) only and do not necessarily reflect those of the European Union. Neither the European Union nor the granting authority can be held responsible for them.

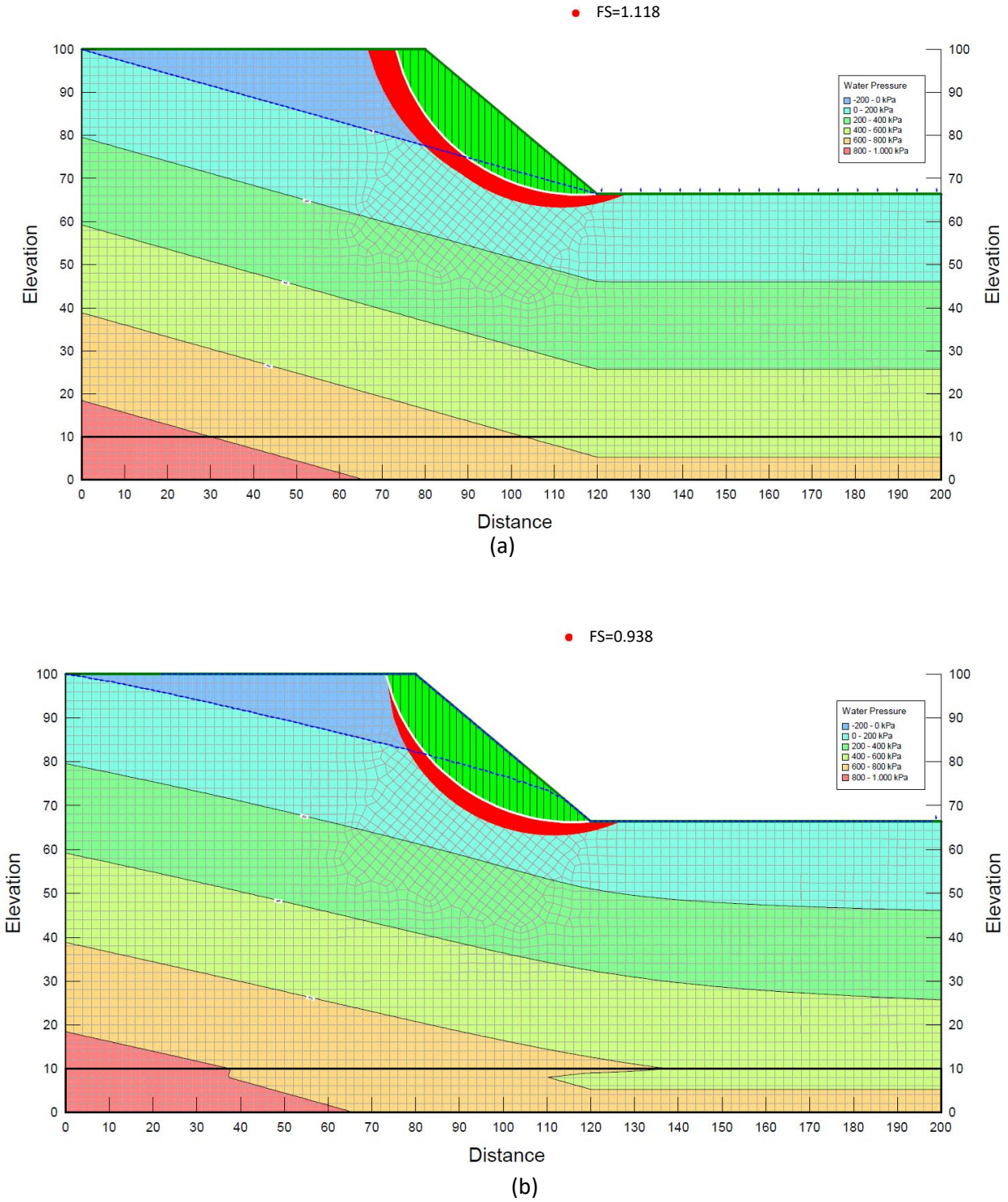

Figure 2.7: (a) Base scenario without precipitation; (b) precipitation with a 30-year return period.

Funded by the European Union. Views and opinions expressed are however those of the author(s) only and do not necessarily reflect those of the European Union. Neither the European Union nor the granting authority can be held responsible for them.

2.2. RISK ASSESSMENT

Landslide Risk can be quantified based on the hazard level and the consequences on infrastructures (i.e., property) and people potentially involved, encompassing both vulnerability assessment and exposure level of the elements at risk.
The description of the quantitative hazard assessment performed for the reference slope elements is reported in Sections 2.1. and 2.2. It describes the criteria and procedures to evaluate the landslide risk for a potentially involved existing area..

2.2.1 Overview: consequences on property and people

The characterization of consequence scenarios for a landslide is based on elements at risk and their vulnerability. The classification of landslide risk elements is still quite preliminary compared to other risks (Cascini et al., 2005) and is mainly based on land use, such as urban, industrial, infrastructural or agricultural land (Calcaterra et al., 2003; Remondo et al., 2003), or considers more detailed structural analyses of buildings that require specialized skills (Spence et al., 2004). The damage of the exposed elements can be structural, bodily and operational (see, for example, Leone et al., 1996).

According to Walker et al. (2007), a quantitative evaluation of the elements at risk includes· property, people, who either live, work, or may spend some time in the area affected by landslide, services, such as water supply or drainage or electricity supply, roads and communication facilities, and vehicles on roads.

Vulnerability is the degree of loss of an element within the landslide affected area (Fell, 1994). While the procedures that assess the resistance and vulnerability to earthquakes and floods are relatively well established and accepted, the assessment of vulnerability of the elements at risk (e.g. buildings, people) to landslides still requires significant efforts in terms of definition and grading (Cascini et al. 2005).
Landslide Risk can be quantified based on the hazard level and the consequences on infrastructures (i.e., property) and people potentially involved, encompassing both vulnerability assessment and exposure level of the elements at risk.
The description of the quantitative hazard assessment performed for the reference slope elements is reported in Sections 2.1. and 2.2. It describes the criteria and procedures to evaluate the landslide risk for a potentially involved existing area.

In particular, the *assessment of landslide consequences for property* must include an estimate of the extent of damage that may affect assets due to the landslide event. The quantitative and accurate assessment of vulnerability can only be carried out on a very detailed scale, where well-documented landslides are available, along with data regarding properties.

Funded by the European Union. Views and opinions expressed are however those of the author(s) only and do not necessarily reflect those of the European Union. Neither the European Union nor the granting authority can be held responsible for them.

Consequences are often calculated using the vulnerability of elements at risk from landslides. The factors that most influence the vulnerability of a property include:

- The volume of the landslide body in relation to the element at risk.
- The position of the element at risk, for example, on the slide or immediately downslope.
- The magnitude of the landslide displacement and the relative movements within the landslide (for elements located on the slide).
- The speed of movement of the landslide body.

Vulnerability of the property quantifies the degree of damage (or monetary loss, in absolute or relative terms) expected to occur in the event of a landslide. The assessment process relies on a quantitative estimation of the projected damage costs, necessitating familiarity with indicative costs for construction and remediation measures. These include direct repair costs, covering restoration of affected structural components and land, stabilization interventions, ensuring site reinforcement to achieve a tolerable risk threshold for landslides, and consequential costs, encompassing indirect economic impacts resulting from the hazard event. Table 2.10 shows the qualitative measures of consequences to property suggested by the *Australian Practice Note Guidelines For Landslide Risk Management* (Walker et al., 2007).

Tab 2.10. Qualitative measures of consequences to property (from Walker et al., 2007).

Approximate Cost of Damage		Description	Descriptor	Level
Indicative Value	Notional Boundary			
200%	100%	Structure(s) completely destroyed and/or large scale damage requiring major engineering works for stabilisation. Could cause at least one adjacent property major consequence damage.	CATASTROPHIC	1
60%	40%	Extensive damage to most of structure, and/or extending beyond site boundaries requiring significant stabilisation works. Could cause at least one adjacent property medium consequence damage.	MAJOR	2
20%	10%	Moderate damage to some of structure, and/or significant part of site requiring large stabilisation works. Could cause at least one adjacent property minor consequence damage.	MEDIUM	3
5%	1%	Limited damage to part of structure, and/or part of site requiring some reinstatement stabilisation works.	MINOR	4
0.5%		Little damage. (Note for high probability event (Almost Certain), this category may be subdivided at a notional boundary of 0.1%. See Risk Matrix.)	INSIGNIFICANT	5

Notes: (2) The Approximate Cost of Damage is expressed as a percentage of market value, being the cost of the improved value of the unaffected property which includes the land plus the unaffected structures.
(3) The Approximate Cost is to be an estimate of the direct cost of the damage, such as the cost of reinstatement of the damaged portion of the property (land plus structures), stabilisation works required to render the site to tolerable risk level for the landslide which has occurred and professional design fees, and consequential costs such as legal fees, temporary accommodation. It does not include additional stabilisation works to address other landslides which may affect the property.
(4) The table should be used from left to right; use Approximate Cost of Damage or Description to assign Descriptor, not vice versa

The *assessment of landslide consequences for people* depends on various factors that influence the risk of injury and mortality, such as the volume of the landslide, the speed of movement, the depth, the burial potential and the exposure conditions (inside or outside the structure involved). Structural integrity is also critical, as the collapse of buildings affects people's vulnerability. People are at the highest risk in the event of a complete structural failure, but even small landslides can cause serious injury to people. Table 2.11 provides some indicative examples of vulnerability values on people, suggested Walker et al. (2007).

Funded by the European Union. Views and opinions expressed are however those of the author(s) only and do not necessarily reflect those of the European Union. Neither the European Union nor the granting authority can be held responsible for them.

Tab 2.11. Qualitative examples of vulnerability values on people (from Walker et al., 2007).

Case	Range in Data	Recommended Value	Comments
Person in Open Space			
If struck by a rockfall	0.1 – 0.7	0.5	May be injured but unlikely to cause death
If buried by debris	0.8 – 1.0	1.0	Death by asphyxia almost certain
If not buried	0.1 – 0.5	0.1	High chance of survival
Persons in a Vehicle			
If the vehicle is buried/crushed	0.9 – 1.0	1.0	Death is almost certain
If the vehicle is damaged only	0 – 0.3	0.3	High chance of survival
Person in a Building			
If the building collapses	0.9 – 1.0	1.0	Death is almost certain
If the building is inundated with debris and the person buried	0.8 – 1.0	1.0	Death is highly likely
If the debris strikes the building only	0 – 0.1	0.05	Very high chance of survival

An example of a qualitative risk matrix used to assess property risk is provided in Walker et al. (2007), and depicted in Table 2.12. This includes a qualitative risk analysis matrix that evaluates the risk level to properties based on qualitative assessments of landslide likelihood and property consequences, along with a matrix indicating the implications of each risk level.

Tab 2.12. Qualitative risk analysis matrix: level of risk to property and risk level implications (from Walker et al., 2007).

QUALITATIVE RISK ANALYSIS MATRIX – LEVEL OF RISK TO PROPERTY

LIKELIHOOD		CONSEQUENCES TO PROPERTY (With Indicative Approximate Cost of Damage)				
	Indicative Value of Approximate Annual Probability	1: CATASTROPHIC 200%	2: MAJOR 60%	3: MEDIUM 20%	4: MINOR 5%	5: INSIGNIFICANT 0.5%
A – ALMOST CERTAIN	10^{-1}	VH	VH	VH	H	M or L (5)
B - LIKELY	10^{-2}	VH	VH	H	M	L
C - POSSIBLE	10^{-3}	VH	H	M	M	VL
D - UNLIKELY	10^{-4}	H	M	L	L	VL
E - RARE	10^{-5}	M	L	L	VL	VL
F - BARELY CREDIBLE	10^{-6}	L	VL	VL	VL	VL

Notes: (5) For Cell A5, may be subdivided such that a consequence of less than 0.1% is Low Risk.
(6) When considering a risk assessment it must be clearly stated whether it is for existing conditions or with risk control measures which may not be implemented at the current time.

RISK LEVEL IMPLICATIONS

Risk Level		Example Implications (7)
VH	VERY HIGH RISK	Unacceptable without treatment. Extensive detailed investigation and research, planning and implementation of treatment options essential to reduce risk to Low; may be too expensive and not practical. Work likely to cost more than value of the property.
H	HIGH RISK	Unacceptable without treatment. Detailed investigation, planning and implementation of treatment options required to reduce risk to Low. Work would cost a substantial sum in relation to the value of the property.
M	MODERATE RISK	May be tolerated in certain circumstances (subject to regulator's approval) but requires investigation, planning and implementation of treatment options to reduce the risk to Low. Treatment options to reduce to Low risk should be implemented as soon as practicable.
L	LOW RISK	Usually acceptable to regulators. Where treatment has been required to reduce the risk to this level, ongoing maintenance is required.
VL	VERY LOW RISK	Acceptable. Manage by normal slope maintenance procedures.

Note: (7) The implications for a particular situation are to be determined by all parties to the risk assessment and may depend on the nature of the property at risk; these are only given as a general guide.

Funded by the European Union. Views and opinions expressed are however those of the author(s) only and do not necessarily reflect those of the European Union. Neither the European Union nor the granting authority can be held responsible for them.

2.2.2. Risk matrix definition

Based on the overview of the literature briefly outlined above, risk matrices were defined that can be used for landslide risk assessment in existing areas. The results of the hazard assessment analyses in terms of the damage parameters (DPs) were combined with a qualitative assessment of the consequences on properties and people involved, in order to obtain reliable results in terms of risk assessment for an existing area, potentially involved by the landslide of a slope.
A risk matrix was defined based on the following information:

- the results of stability analyses of the reference slopes described in the previous paragraph in terms of safety factors (*FoS*), and the maximum depths of the critical slip surface (z_s);
- the return periods of climatic events corresponding to the *FoS* values;
- the presence of "property" (e.g. structures, infrastructures) near the slope and the distance of property from the slope;
- the presence of people;
- the level of consequences on structures and people may face.

Risk matrix definition involves the following steps.

Step 1. Numerical evaluation of FoS_i

First, as described in Section 2.1, for each reference slope, a set of 4 hydro-mechanical numerical analyses were performed using Seep/W and Slope/W codes, considering 4 different inputs in terms of reference climate events and obtaining 4 different values of the factor of safety (FoS_i):

- the first simulation was carried out without considering any rainfall events, whose results led to a *FoS* value referred to as FoS_0;
- the second simulation took into account a rainfall event with a return period of 30 years, resulting in a *FoS* value referred to as FoS_1;
- the third simulation considered the effects of a rainfall event with a 200-year return period, yielding a corresponding *FoS* value referred to as FoS_2;
- the fourth simulation accounted for the influence of a rainfall event with a 500-year return period, resulting in a *FoS* value indicated as FoS_3.

Table 2.13 shows the set of analyses for each reference slope, along with the return period of the input rainfall, the annual probability of occurrence of the rainfall, and the name of the calculated factor of safety of the slope, for each simulation.

Funded by the European Union. Views and opinions expressed are however those of the author(s) only and do not necessarily reflect those of the European Union. Neither the European Union nor the granting authority can be held responsible for them.

Tab 2.13. Set of analyses for each reference slope for different rainfalls.

Simulation	**rainfall event return period Tr** (years)	**Annual probability of occurrence**	***FoS$_i$***
1	no rainfall	-	*FoS$_0$*
2	30	3.3E-02	*FoS$_1$*
3	200	5.0E-03	*FoS$_2$*
4	500	2.0E-03	*FoS$_3$*

According to the Eurocode 7 (1997), design values of the soil mechanical parameters were adopted in FEM analyses. Based on these values of soil parameters, a threshold of *FoS* = 1 was considered to identify the incipient collapse. *FoS* values higher than 1 indicate stable slope conditions; *FoS* values lower than or equal to 1 indicate instability.

Step 2. Definition of the hazard levels

In the next step, for a given reference slope, different hazard levels have been defined based on the values of the four different factors of safety (*FoS$_i$*) obtained for the different return periods (or annual probability of occurrence) of the rainfalls, as indicated in Tab. 2.14.

Tab 2.14. Definition of the level of hazard based on the *FoS$_i$* values.

FoS$_0$ no rainfall	***FoS$_1$*** T_r=30 years	***FoS$_2$*** T_r=200 years	***FoS$_3$*** T_r=500 years	**Hazard levels**
<=1	<=1	<=1	<=1	Very high (landslide certain)
>1	<=1	<=1	<=1	High (almost certain)
>1	>1	<=1	<=1	Medium (likely)
>1	>1	>1	<=1	Low (unlikely)
>1	>1	>1	>1	Very low (almost null)

According to the procedure of Walker et al. (2007), score values were assigned to the five different hazard levels, increasing with the significance of the hazard, as indicated in Table 2.15.

Co-funded by the European Union
Funded by the European Union. Views and opinions expressed are however those of the author(s) only and do not necessarily reflect those of the European Union. Neither the European Union nor the granting authority can be held responsible for them.

Table 2.15. Scores assigned to the different hazard levels.

Landslide Hazard Level	Very high (landslide certain)	1
	High (almost certain)	0.8
	Medium (likely)	0.6
	Low (unlikely)	0.3
	Very low (almost null)	0.1

Step 3. Evaluation of the consequences on properties and people

In the following step, the consequences for property and people were assessed, based on two significant key parameters:

- the position of the structure/infrastructure relative to the landslide body;
- the significance of the landslide.

Damage levels caused by the occurrence of a landslide were defined based on the residual operational capacity of a built system and the people involved.

The following five damage levels were established:

- *Very high* (D5). Complete destruction of structures/infrastructures, large-scale damage. 100% loss of human life. Reconstruction through major engineering works and stabilization.
- *High* (D4). Severe damage to structures/infrastructures within and adjacent to the site. Irreversible damage to the construction system (reinforced concrete frame and masonry walls). 80% loss of human life for structures/infrastructures within the site and 60% for adjacent structures/infrastructures. Evacuation required. Possible long-term use of structures, with significant reconstruction and stabilization interventions.
- *Medium* (D3). Moderate to severe damage to structures/infrastructures within and adjacent to the site. Damage to individual parts of the construction system (nodes, columns, beams, reinforced concrete elements, openings, and rotations causing deformations in masonry walls), as well as secondary construction elements (reinforced concrete paneling and cracks in masonry structures). Inability to use several floors due to debris presence. 60% loss of human life for structures/infrastructures within the site and 40% for adjacent ones. Evacuation suggested. Possible long-term use of structures, only with significant reconstruction and stabilization interventions.
- Low (D2). Moderate and limited damage to structures within the site. Damage to secondary elements of the construction system (reinforced concrete paneling and cracks in masonry structures). Inability to use several floors due to debris presence. 40% loss of human life. No evacuation required. Possible short-term use of structures. Inspection necessary for potential limited reconstruction and stabilization interventions.
- Very low (D1). Minimal damage. Immediate stability and usability of structures following

Funded by the European Union. Views and opinions expressed are however those of the author(s) only and do not necessarily reflect those of the European Union. Neither the European Union nor the granting authority can be held responsible for them.

inspection. No evacuation required.

Five consequences levels are considered corresponding to these five damage levels:

- Damage level D5 - Very High consequences;
- Damage level D4 - High consequences;
- Damage level D3 - Medium consequences;
- Damage level D2 -Low consequences;
- Damage level D1 - Very Low consequences.

Scores increasing in proportion to the expected damage were assigned to each level of damage/consequences, as indicated in Tab. 2.16.

Table 2.16. Scores assigned to the different levels of damage/consequences (adapted from Leone et al., 1996).

Assigned scores to damage levels/consequences on property and people				
VERY HIGH D5 level	HIGH D4 level	MEDIUM D3 level	LOW D2 level	VERY LOW D1 level
1	0.8	0.6	0.3	0.1

In order to associate the five damage levels to a given property located in an area potentially involved by a landslide event, two key parameters - the *relative position of the property* and the *significance* of the landslide must be considered.

Regarding the *position of the property in relation to the slope*, we considered four possible locations, based on the distance of the property from the slope (see the geometrical details in Fig. 2.8):

- *On*: property located on the slope ($x < L$)
- *Adjacent*: property adjacent to the slope affected by the landslide event ($x \geq L$ and $z_s/x > 0.4$)
- *Near*: property near the slope affected by the landslide ($x \geq L$ and $0.1 < z_s/x \leq 0.4$)
- *Out*: property not affected by the event ($x \geq L$ and $z_s/x \leq 0.1$).

Co-funded by the European Union

Funded by the European Union. Views and opinions expressed are however those of the author(s) only and do not necessarily reflect those of the European Union. Neither the European Union nor the granting authority can be held responsible for them.

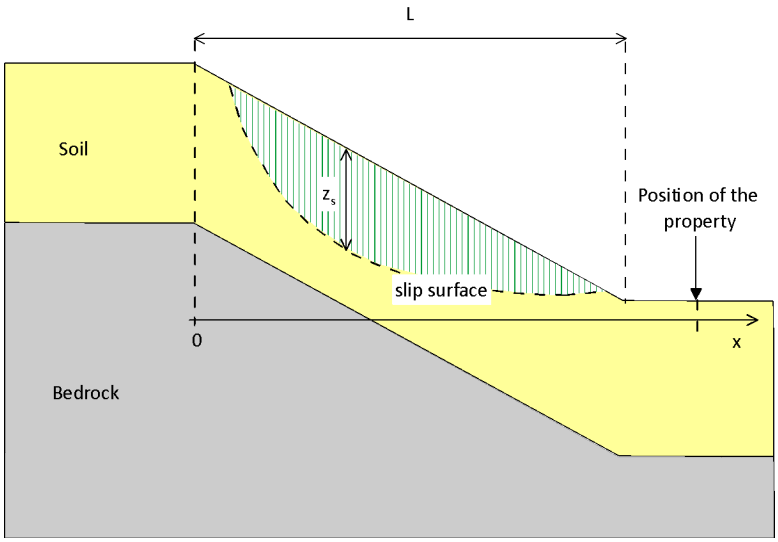

Figure 2.8. Schematic representations of the position of the property.

The *significance of the potential landslide* was assumed to be related to the maximum depth of the sliding surface (z_s). This can be justified since the considered rainfall-induced slope landslides in soils are characterized by circular slip surfaces, and landslides become more significant in terms of potential damage the deeper they are.
Four significance levels were defined:

- Very deep sliding surface ($z_s > 15$ m) – high significance
- Deep (10 m < $z_s \leq 15$ m) – moderately high significance
- Intermediate (5 m < $z_s \leq 10$ m) – medium significance
- Shallow ($z_s \leq 5$ m) – low significance

Based on these definitions, the association of five damage levels to the different combinations of the two key parameters – e.g., landslide's significance and property's position - is shown in Tab. 2.17.

Table 2.17. Definition of the levels of damage based on the significance of the landslide and the position of the property.

	On	**Adjacent**	**Near**	**Out**
Very deep $z_s > 15$ m	D5	D5	D4	D2
Deep 10 m < $z_s \leq 15$ m	D5	D4	D3	D2
Intermediate 5 m < $z_s \leq 10$ m	D5	D4	D3	D1
Shallow $z_s \leq 5$ m	D4	D3	D2	D1

Co-funded by the European Union
Funded by the European Union. Views and opinions expressed are however those of the author(s) only and do not necessarily reflect those of the European Union. Neither the European Union nor the granting authority can be held responsible for them.

Step 4. Definition of the risk matrix

Finally, by combining the hazard levels with the damage levels obtained through the procedures described above, the criteria to define the risk matrix can be evaluated (Tab. 2.18). In this matrix, the risk indicator in each cell is obtained by multiplying the score related to the hazard by the one related to the consequences.

Table 2.18. Definition of the criteria to determine the risk matrix

			qualitative measure of consequences to PROPERTY				
			CATASTROPHIC structure destroyed	MAJOR extensive damage	MEDIUM moderate damage	MINOR limited damage	INSIGNIFICANT little damage
			1	0.8	0.6	0.3	0.1
HAZARD	certain	1	**1.00**	**0.80**	**0.60**	**0.30**	**0.10**
	almost certain	0.8	**0.80**	**0.64**	**0.48**	**0.24**	**0.08**
	likely	0.6	**0.60**	**0.48**	**0.36**	**0.18**	**0.06**
	possible	0.3	**0.30**	**0.24**	**0.18**	**0.09**	**0.03**
	unlikely	0.1	**0.10**	**0.08**	**0.06**	**0.03**	**0.01**

Based on the values of the risk indicators, five distinct risk classes were defined. In particular:

- Very high risk level (**VH**) – score ≥0.7 (red)
- High risk level (**H**) – 0.5 ≤ score < 0.7 (orange)
- Medium risk level (**M**) - 0.3 ≤ score < 0.5 (yellow)
- Low risk level (**L**) - 0.1 ≤ score < 0.3 (light blue)
- Very Low risk level (**VL**) - score <0.1 (light green)

Co-funded by the European Union

Funded by the European Union. Views and opinions expressed are however those of the author(s) only and do not necessarily reflect those of the European Union. Neither the European Union nor the granting authority can be held responsible for them.

Table 2.19 is the final qualitative **risk matrix**, where colors correspond to the different classes of risk.

Table 2.19. Risk matrix

		Level of consequences				
		Very High	High	Medium	Low	Very Low
HAZARD	Very High	**VH**	**VH**	**H**	**M**	**L**
	High	**VH**	**H**	**M**	**L**	**VL**
	Medium	**H**	**M**	**M**	**L**	**VL**
	Low	**M**	**L**	**L**	**VL**	**VL**
	Very low	**L**	**VL**	**VL**	**VL**	**VL**

Funded by the European Union. Views and opinions expressed are however those of the author(s) only and do not necessarily reflect those of the European Union. Neither the European Union nor the granting authority can be held responsible for them.

3. FLOODING RISK ASSESSMENT OF REFERENCE ELEMENTS (RIVERS)

3.1. REFERENCE SCENARIOS

To provide representative conditions for the river reference element, we considered scenarios involving different combinations of the following parameters:

- Rainfall return period
- Drainage basin Area
- Mean slope of the drainage basin
- Mean slope of the river
- Mean slope of the floodplain

The mean slope of the drainage basin was classified as low (L), medium (M) and high (H). Likewise, for the mean slope of the river and floodplain, three slope categories were identified, termed L, M and H for rivers, and LL, MM and HH for floodplains (considering the two directions in the plan), respectively. In addition, a triangular shape of the hydrograph was assumed, and typical values of the runoff coefficient c and the roughness coefficient, which were kept constant in the performed simulations.
After estimating the time of concentration Tc and, consequently, the rainfall intensity pertaining to different scenarios, the peak discharge Q_{max} was calculated by adopting the simple rational method and considering a correction factor depending on the extension of the drainage basin area A (Chow et al., 1988; Bedient et al., 2012).

Specifically, the peak discharge Q_{max} is evaluated using the following equation accounting for areal effects (this formula is consistent with data from several Italian catchments – see also Arno River Basin Authority):

$$Q_{max} = Q_0[-0.116lnA + 1.1088] \quad (1)$$

where A is the drainage basin area [in km^2] and

$$Q_0 = chA/T_c \quad (2)$$

is the discharge calculated using the rational method, with c indicating the runoff coefficient, and h represents the rainfall height. Note that the rainfall intensity is $i=h/T_c$.

The concentration time T_c can be estimated as follows:

$$T_c = [4A^{0.5} + 1.5L]/(0.8H_m^{0.5}) \quad (3)$$

Funded by the European Union. Views and opinions expressed are however those of the author(s) only and do not necessarily reflect those of the European Union. Neither the European Union nor the granting authority can be held responsible for them.

where *L* indicates the length of the flow path and *Hm* is the mean elevation of the drainage basin.

Assuming $t=T_c$, the rainfall height *h* in Eq. (2) is calculated using the following depth-duration-frequency relationship pertaining to the reference climate event:

$$h = at^n T_r^m \quad (4)$$

where *a* is a coefficient, *t* is the time (in hours) and *Tr* is the return period of the rainfall event (in years). From hydrological analyses, we derived the following values: *a* = 26, *n* = 0.38 and *m* = 0.22.

The Chicago hyetograph was adopted as the design hyetograph (see Fig. 2.4).By using the software HEC-RAS and assuming the location for the break point on the floodplain, i.e., the point where flow spills from the main river channel onto the floodplain, the flood areas were calculated. In this regard, it is worth remarking that the flow has been simulated as one-dimensional and unsteady in the river and as fully unsteady and two-dimensional in the floodplains. The Manning coefficient has been assumed to be equal to 0.04 in the river and 0.06 on the floodplains.

The results pertaining to each simulated scenario were reported in geoTIFF files showing the maximum depth of the water [m], the maximum velocity [m/s] and the arrival time of the water (hours). The floodplain used in the simulation was a square surface whose area is 5x5 km^2, with respectively zero slope (LL), 0,1% slope (MM) and 1% slope (HH) in both the directions of the plane.

In the following, a table is reported that summarize the main input and output parameters, along with the results obtained from the simulations. More specifically, in this table *c* [-] is the runoff coefficient, a, n, m are the parameters of the depth-duration-frequency curve pertaining to the reference climate event (Eq. 4). *A* [km^2] is the drainage basin area, *L* [km] is the estimated length of the flow path within the drainage basin, *I* [-] is the drainage basin mean slope, *Hm* [m] is the mean elevation of the drainage basin, *Tc* [hours] is the estimated time of concentration, *Tr* [years] is the return period of the rainfall, i [mm/hour] is the rainfall intensity and *Qmax* [m^3/s] is the peak discharge.

The code for river and floodplain slopes should be interpreted as follows. For instance, the code MMM refers to the medium river slope (M) and to the medium floodplain slope (MM). Likewise, an intuitive nomenclature was also adopted for the code of simulated scenarios. For instance, A2-MMM-TR010 refers to the simulated scenario with *A* = 2 km^2 (A2), medium slope of the river (M), medium slope of the floodplain (MM), and TR010 means that the return period is *Tr*=10

Funded by the European Union. Views and opinions expressed are however those of the author(s) only and do not necessarily reflect those of the European Union. Neither the European Union nor the granting authority can be held responsible for them.

years.

Table 3.1. Example of simulated scenarios with relative input and output parameters.

		Parameters of the depth-duration-frequency curve			Parameters of the drainage basin										
Code for the simulated scenario	Runoff coefficient c	a	n	m	Drainage basin area A (km^2)	Lenght of the flow path within the drainage basin L (km)	Code for the drainage basin mean slope	Drainage basin mean slope I	Mean elevation of the drainage basin Hm [m]	Time of concentration Tc [hours]	Return period of the rainfall Tr [years]	Rainfall intensity i [mm/h]	Peak discharge Q_{max} [m^3/s]	Code for river and flood plain slopes	Result of the simulation
A2-MMM-TR010	0.4	26	0.38	0.22	2	2.00	M	0.04	20.00	2.42	10	24.95	20.5	MMM	
A2-MMM-TR030	0.4	26	0.38	0.22	2	2.00	M	0.04	20.00	2.42	30	31.77	26.1	MMM	
A2-MMM-TR100	0.4	26	0.38	0.22	2	2.00	M	0.04	20.00	2.42	100	41.40	34.1	MMM	
A2-MMM-TR200	0.4	26	0.38	0.22	2	2.00	M	0.04	20.00	2.42	200	48.22	39.7	MMM	
A2-MHH-TR010	0.4	26	0.38	0.22	2	2.00	M	0.04	20.00	2.42	10	24.95	20.5	MHH	
A2-MHH-TR030	0.4	26	0.38	0.22	2	2.00	M	0.04	20.00	2.42	30	31.77	26.1	MHH	
A2-MHH-TR100	0.4	26	0.38	0.22	2	2.00	M	0.04	20.00	2.42	100	41.40	34.1	MHH	
A2-MHH-TR200	0.4	26	0.38	0.22	2	2.00	M	0.04	20.00	2.42	200	48.22	39.7	MHH	
A2-LLL-TR010	0.4	26	0.38	0.22	2	2.00	L	0.01	4.00	5.41	10	15.15	12.5	LLL	
A2-LLL-TR030	0.4	26	0.38	0.22	2	2.00	L	0.01	4.00	5.41	30	19.29	15.9	LLL	
A2-LLL-TR100	0.4	26	0.38	0.22	2	2.00	L	0.01	4.00	5.41	100	25.14	20.7	LLL	
A2-LLL-TR200	0.4	26	0.38	0.22	2	2.00	L	0.01	4.00	5.41	200	29.28	24.1	LLL	
A10-MMM-TR010	0.4	26	0.38	0.22	10	4.47	M	0.04	44.72	3.62	10	19.44	65.5	MMM	
A10-MMM-TR030	0.4	26	0.38	0.22	10	4.47	M	0.04	44.72	3.62	30	24.76	83.3	MMM	
A10-MMM-TR100	0.4	26	0.38	0.22	10	4.47	M	0.04	44.72	3.62	100	32.26	108.6	MMM	
A10-MMM-TR200	0.4	26	0.38	0.22	10	4.47	M	0.04	44.72	3.62	200	37.58	126.5	MMM	
A10-MHH-TR010	0.4	26	0.38	0.22	10	4.47	M	0.04	44.72	3.62	10	19.44	65.5	MHH	
A10-MHH-TR030	0.4	26	0.38	0.22	10	4.47	M	0.04	44.72	3.62	30	24.76	83.3	MHH	
A10-MHH-TR100	0.4	26	0.38	0.22	10	4.47	M	0.04	44.72	3.62	100	32.26	108.6	MHH	
A10-MHH-TR200	0.4	26	0.38	0.22	10	4.47	M	0.04	44.72	3.62	200	37.58	126.5	MHH	
A10-LLL-TR010	0.4	26	0.38	0.22	10	4.47	L	0.01	8.94	8.09	10	11.80	39.7	LLL	
A10-LLL-TR030	0.4	26	0.38	0.22	10	4.47	L	0.01	8.94	8.09	30	15.03	50.6	LLL	
A10-LLL-TR100	0.4	26	0.38	0.22	10	4.47	L	0.01	8.94	8.09	100	19.59	66.0	LLL	
A10-LLL-TR200	0.4	26	0.38	0.22	10	4.47	L	0.01	8.94	8.09	200	22.82	76.8	LLL	
A100-MMM-TR010	0.4	26	0.38	0.22	100	14.14	M	0.04	141.42	6.43	10	13.61	312.7	MMM	
A100-MMM-TR030	0.4	26	0.38	0.22	100	14.14	M	0.04	141.42	6.43	30	17.32	398.2	MMM	
A100-MMM-TR100	0.4	26	0.38	0.22	100	14.14	M	0.04	141.42	6.43	100	22.58	519.0	MMM	
A100-MMM-TR200	0.4	26	0.38	0.22	100	14.14	M	0.04	141.42	6.43	200	26.30	604.4	MMM	
A100-MHH-TR010	0.4	26	0.38	0.22	100	14.14	M	0.04	141.42	6.43	10	13.61	312.7	MHH	GeoTIFF maps with the location of the breakpoint, velocity of flow, water depths and arrival time
A100-MHH-TR030	0.4	26	0.38	0.22	100	14.14	M	0.04	141.42	6.43	30	17.32	398.2	MHH	
A100-MHH-TR100	0.4	26	0.38	0.22	100	14.14	M	0.04	141.42	6.43	100	22.58	519.0	MHH	
A100-MHH-TR200	0.4	26	0.38	0.22	100	14.14	M	0.04	141.42	6.43	200	26.30	604.4	MHH	
A100-LLL-TR010	0.4	26	0.38	0.22	100	14.14	L	0.01	28.28	14.39	10	8.26	189.9	LLL	
A100-LLL-TR030	0.4	26	0.38	0.22	100	14.14	L	0.01	28.28	14.39	30	10.52	241.8	LLL	
A100-LLL-TR100	0.4	26	0.38	0.22	100	14.14	L	0.01	28.28	14.39	100	13.71	315.1	LLL	
A100-LLL-TR200	0.4	26	0.38	0.22	100	14.14	L	0.01	28.28	14.39	200	15.97	367.0	LLL	
A1000-MMM-TR010	0.4	26	0.38	0.22	1000	44.72	M	0.04	447.21	11.44	10	9.52	1171.1	MMM	
A1000-MMM-TR030	0.4	26	0.38	0.22	1000	44.72	M	0.04	447.21	11.44	30	12.12	1491.3	MMM	
A1000-MMM-TR100	0.4	26	0.38	0.22	1000	44.72	M	0.04	447.21	11.44	100	15.80	1943.6	MMM	
A1000-MMM-TR200	0.4	26	0.38	0.22	1000	44.72	M	0.04	447.21	11.44	200	18.40	2263.8	MMM	
A1000-MHH-TR010	0.4	26	0.38	0.22	1000	44.72	M	0.04	447.21	11.44	10	9.52	1171.1	MHH	
A1000-MHH-TR030	0.4	26	0.38	0.22	1000	44.72	M	0.04	447.21	11.44	30	12.12	1491.3	MHH	
A1000-MHH-TR100	0.4	26	0.38	0.22	1000	44.72	M	0.04	447.21	11.44	100	15.80	1943.6	MHH	
A1000-MHH-TR200	0.4	26	0.38	0.22	1000	44.72	M	0.04	447.21	11.44	200	18.40	2263.8	MHH	
A1000-LLL-TR010	0.4	26	0.38	0.22	1000	44.72	L	0.01	89.44	25.58	10	5.78	711.1	LLL	
A1000-LLL-TR030	0.4	26	0.38	0.22	1000	44.72	L	0.01	89.44	25.58	30	7.36	905.5	LLL	
A1000-LLL-TR100	0.4	26	0.38	0.22	1000	44.72	L	0.01	89.44	25.58	100	9.59	1180.1	LLL	
A1000-LLL-TR200	0.4	26	0.38	0.22	1000	44.72	L	0.01	89.44	25.58	200	11.18	1374.5	LLL	
A10000-MMM-TR010	0.4	26	0.38	0.22	10000	141.42	M	0.04	1414.21	20.35	10	6.66	2424.8	MMM	
A10000-MMM-TR030	0.4	26	0.38	0.22	10000	141.42	M	0.04	1414.21	20.35	30	8.49	3087.8	MMM	
A10000-MMM-TR100	0.4	26	0.38	0.22	10000	141.42	M	0.04	1414.21	20.35	100	11.06	4024.2	MMM	
A10000-MMM-TR200	0.4	26	0.38	0.22	10000	141.42	M	0.04	1414.21	20.35	200	12.88	4687.1	MMM	
A10000-MHH-TR010	0.4	26	0.38	0.22	10000	141.42	M	0.04	1414.21	20.35	10	6.66	2424.8	MHH	
A10000-MHH-TR030	0.4	26	0.38	0.22	10000	141.42	M	0.04	1414.21	20.35	30	8.49	3087.8	MHH	
A10000-MHH-TR100	0.4	26	0.38	0.22	10000	141.42	M	0.04	1414.21	20.35	100	11.06	4024.2	MHH	
A10000-MHH-TR200	0.4	26	0.38	0.22	10000	141.42	M	0.04	1414.21	20.35	200	12.88	4687.1	MHH	
A10000-LLL-TR010	0.4	26	0.38	0.22	10000	141.42	L	0.01	282.84	45.50	10	4.06	1472.3	LLL	
A10000-LLL-TR030	0.4	26	0.38	0.22	10000	141.42	L	0.01	282.84	45.50	30	5.15	1874.8	LLL	
A10000-LLL-TR100	0.4	26	0.38	0.22	10000	141.42	L	0.01	282.84	45.50	100	6.71	2443.4	LLL	
A10000-LLL-TR200	0.4	26	0.38	0.22	10000	141.42	L	0.01	282.84	45.50	200	7.82	2845.9	LLL	

More specifically, in the following figures are reported examples of outputs obtained from simulations and pertaining to selected scenarios, along with corresponding explanations.

Co-funded by the European Union

Funded by the European Union. Views and opinions expressed are however those of the author(s) only and do not necessarily reflect those of the European Union. Neither the European Union nor the granting authority can be held responsible for them.

It is worth noticing that to avoid any significant influence of boundary conditions on the flow characteristics within the floodplain, these conditions are placed 5 km away from the break points as a normal depth condition, with a slope nearly equal to that of the DTM plane.

The adopted DTMs represent various floodplain configurations. For example, Fig. 3.1 shows a horizontal area (with zero slope in both directions). As can be seen, the ground elevation is nearly constant, ranging from 250 m a.s.l. to 250.1 m a.s.l., where the 250 m value serves merely as a relative reference. Other DTMs with constant slopes in both directions were also used to simulate alternative scenarios.

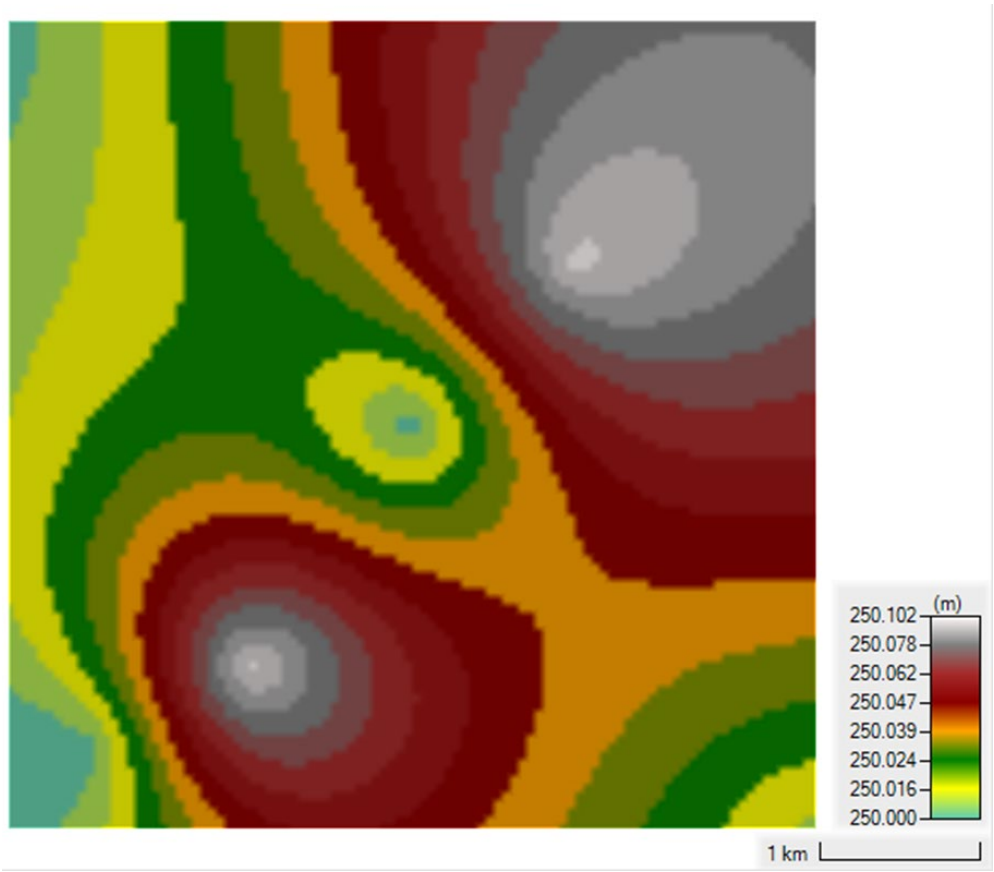

Fig. 3.1 DTM for the horizontal floodplain.

Fig. 3.2 displays the GeoTIFF DTM map, showing the river's location (identified via the cross-section numbers from 101 to 102 indicated on the left vertical axis) and the break points (i.e., from section 101.5 to section 101.7) in the levee pertaining to different scenarios with the slope of river and floodplain very low and equal to 0% (LL).

Funded by the European Union. Views and opinions expressed are however those of the author(s) only and do not necessarily reflect those of the European Union. Neither the European Union nor the granting authority can be held responsible for them.

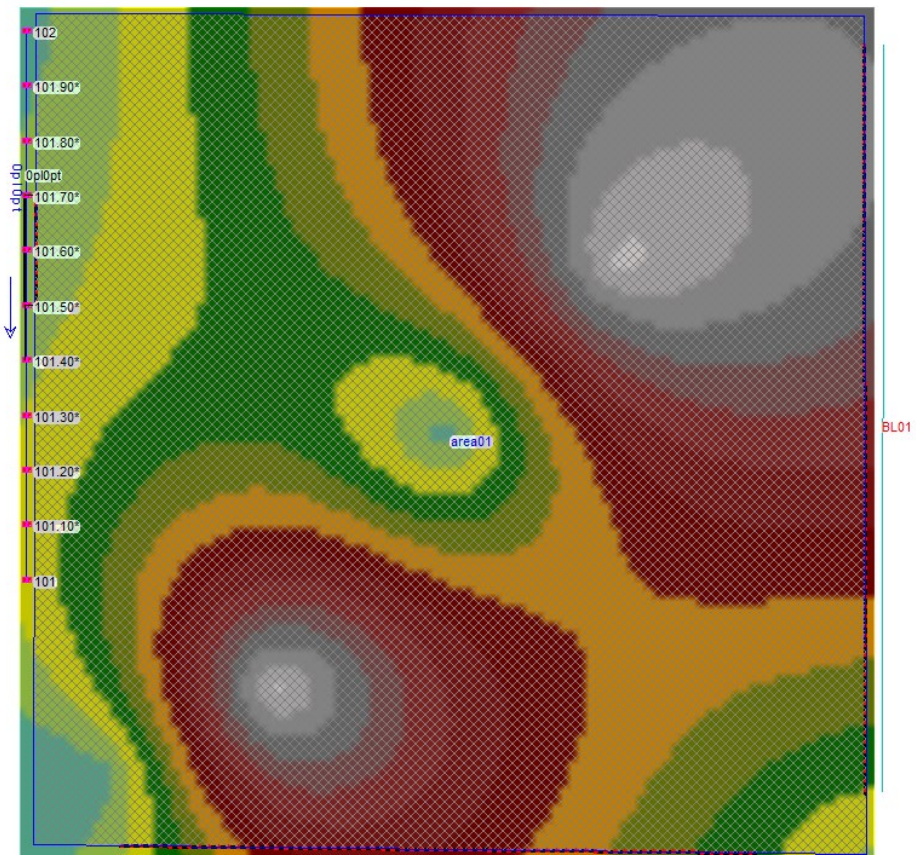

Figure 3.2. GeoTIFF DTM map with the identification of the river (cross-section numbers ranging from 101 to 102 and shown on the left) and the break points (from section 101.5 to section 101.7) in the levee pertaining to different scenarios with the slope of river and floodplain very low and equal to 0% (LL), respectively.

For each simulated scenario, longitudinal profiles of the river and flood hydrographs at different locations are also obtained.

For example, Fig. 3.3 shows the water profile (continuous blue line) relative to the simulation A10000-MHH-Tr100. In this figure, the gray shaded area indicates the overtopped levee (break points) between cross section 101.4 and 101.7. It is worth remarking that flooding occurs only at the overtopped levee (gray shaded area) in the model.

Funded by the European Union. Views and opinions expressed are however those of the author(s) only and do not necessarily reflect those of the European Union. Neither the European Union nor the granting authority can be held responsible for them.

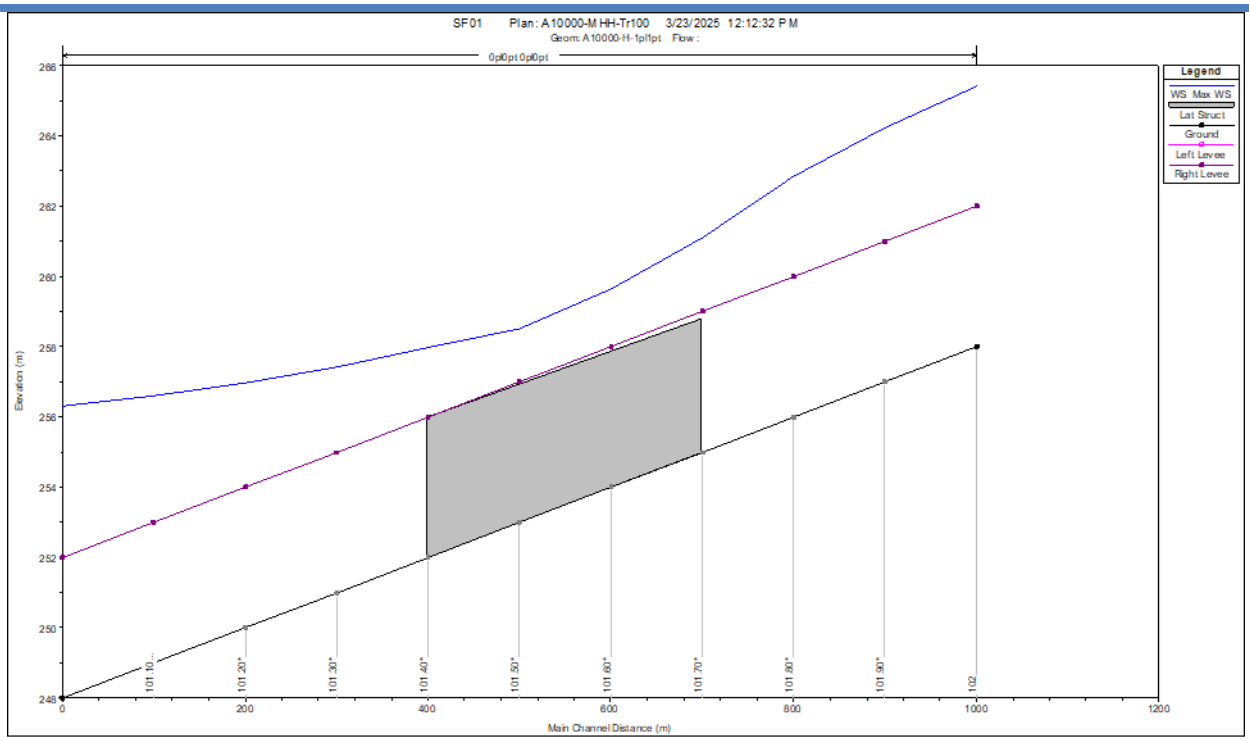

Fig. 3.3 Longitudinal river profile showing the overtopped levee (occurring only between cross section 101.4 and 101.7) for the simulation A10000-MHH-Tr100.

For the same simulation A10000-MHH-Tr100, Fig. 3.4 also illustrates three hydrographs, i.e., upstream, downstream and at the location of the overtopped levee (i.e., the flood hydrograph). Namely, the hydrograph upstream of the overtopped levee has been simulated with a triangular shape and is termed “Flow HW US” in the legend. Likewise, the downstream hydrograph and the flood hydrograph are named “Flow HW DS” and “Weir Flow” in the legend, respectively. (Note that the hydrograph corresponding to “Total flow” in the legend overlaps the upstream hydrograph.)

Funded by the European Union. Views and opinions expressed are however those of the author(s) only and do not necessarily reflect those of the European Union. Neither the European Union nor the granting authority can be held responsible for them.

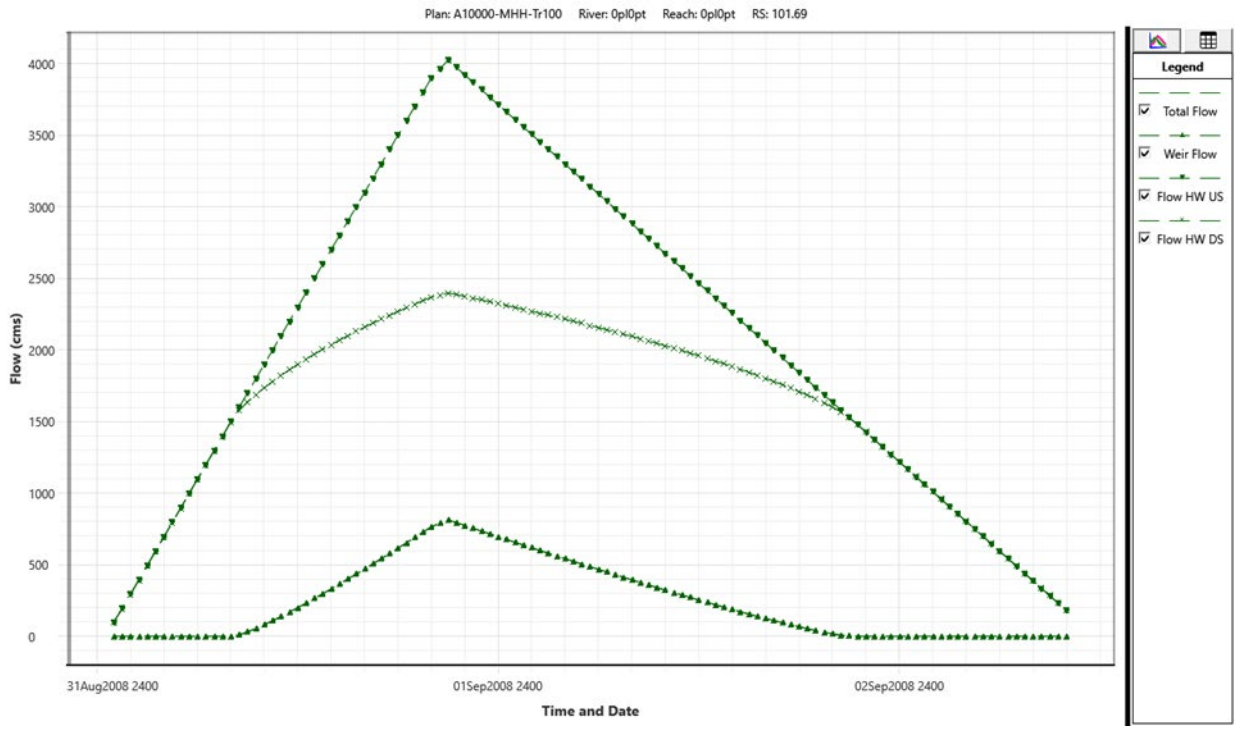

Fig. 3.4 Flood hydrograph (Weir flow) compared to upstream (Flow HW US) and downstream (Flow HW DS) flow hydrographs for simulation A10000-MHH-Tr100.

As mentioned above, for all the simulations, results are given in terms of raster maps of the maximum water depth, max velocity and arrival time.

Some examples are reported below. Specifically, Fig. 3.5 illustrates the envelope of the maximum water depth during the unsteady flow phenomena of flooding pertaining to the simulation A1000-MMM-Tr100. The bold blue line on the left indicates the river, while the location of the levee break point is identified by the red ellipse. It is worth noticing that the maximum water depth varies between 0.5 and 1 m, i.e., it is higher close to the levee and then decreases. Likewise, Fig. 3.6 shows similar results pertaining to the simulation A1000-LLL-Tr100. In this case, the maximum water depth varies between 0.5 and 1 m. Again, higher water depths occur close to the levee and then decrease.

Co-funded by the European Union

Funded by the European Union. Views and opinions expressed are however those of the author(s) only and do not necessarily reflect those of the European Union. Neither the European Union nor the granting authority can be held responsible for them.

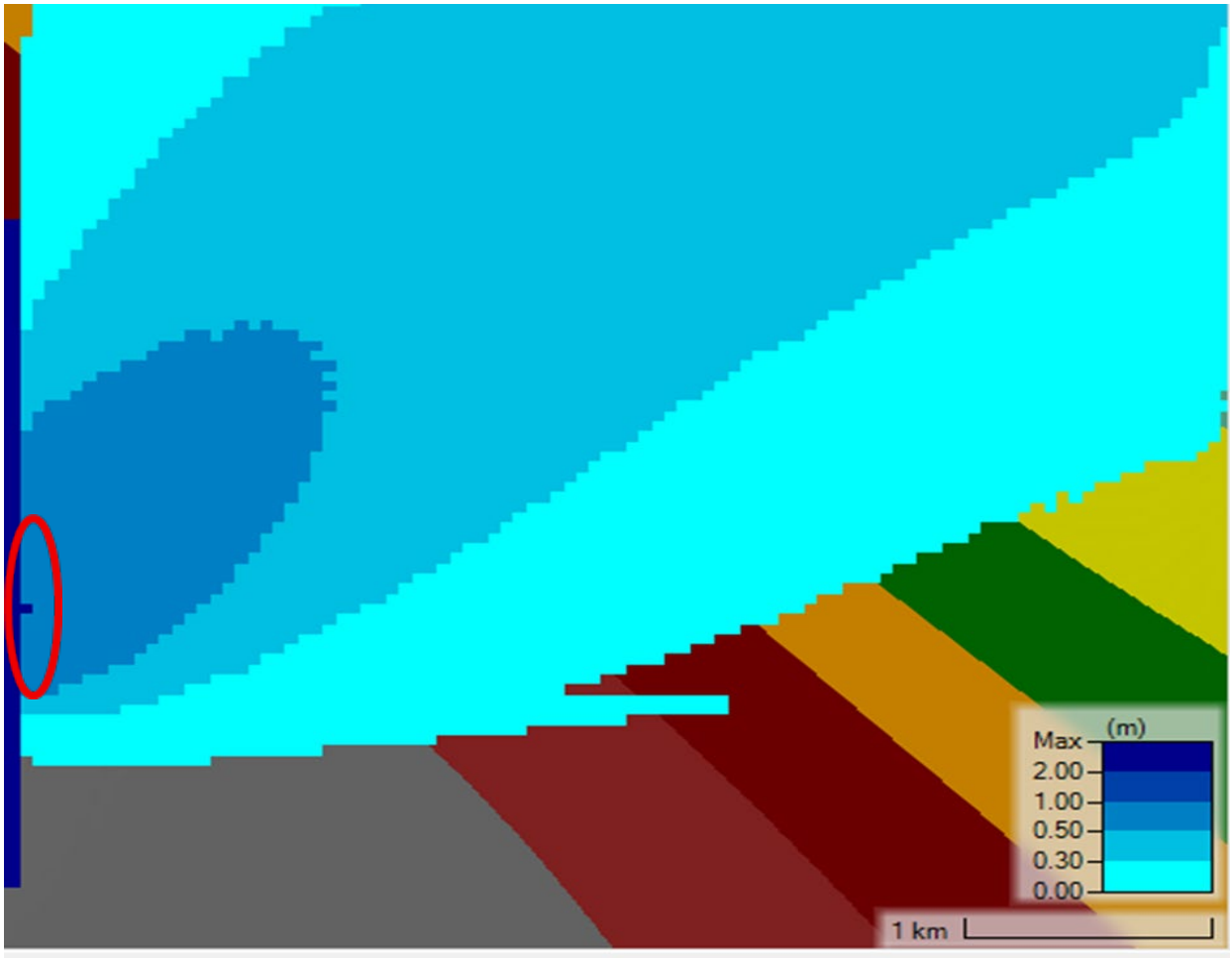

Fig.3.5. Envelope of the maximum water depth for the simulation A1000-MMM-Tr100. The bold blue line on the left indicates the river. The location of the levee break point is identified by the red ellipse. Maximum water depth varies between 0.5 and 1 m.

Funded by the European Union. Views and opinions expressed are however those of the author(s) only and do not necessarily reflect those of the European Union. Neither the European Union nor the granting authority can be held responsible for them.

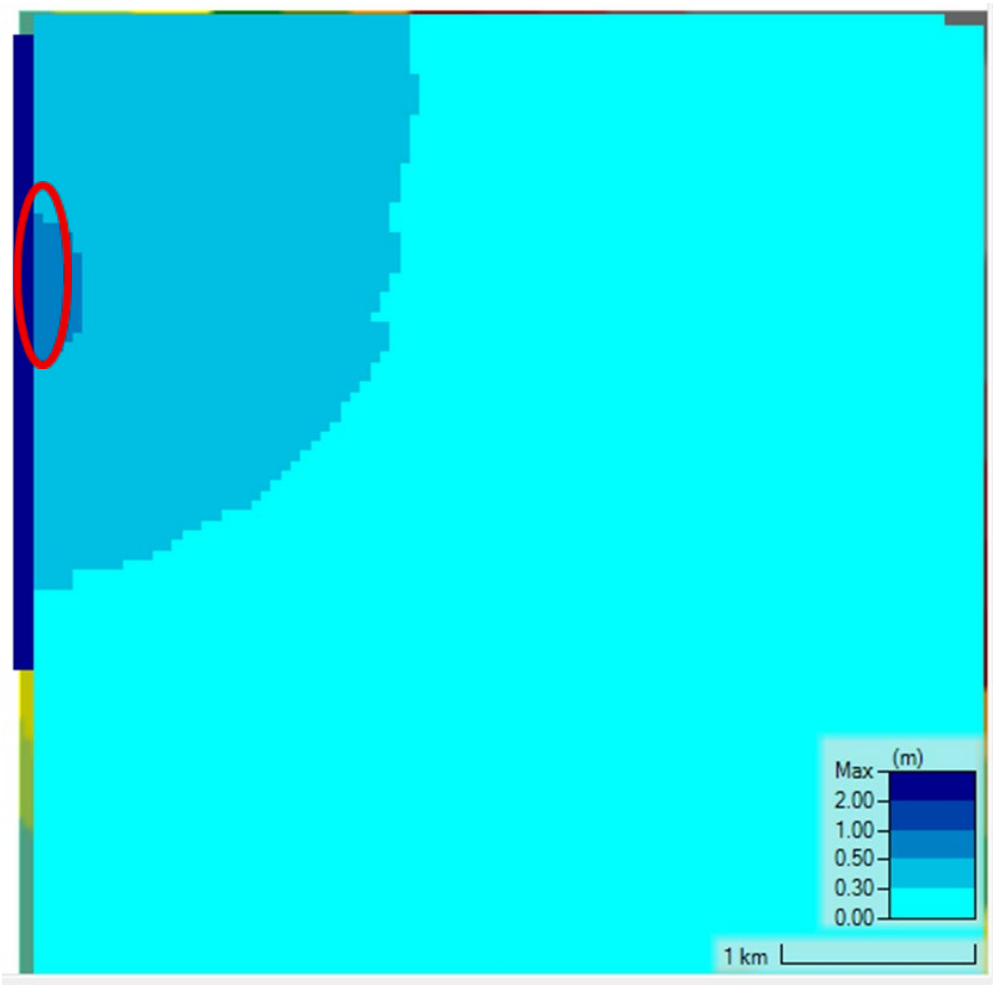

Figure 3.6. Envelope of the maximum water depth for the simulation A1000-LLL-Tr100. The bold blue line on the left indicates the river. The location of the levee break point is identified by the red ellipse. Maximum water depth varies between 0.5 and 1 m.

Results also include GeoTIFF maps illustrating the simulated max water velocity and the arrival time in the floodplain. For instance, from Fig. 3.7, it can be observed that flow velocities are less than approximately 2 m/s in all the flooded area. Likewise, Fig. 3.8 shows the plot of the arrival time after the start of the flood event.

Funded by the European Union. Views and opinions expressed are however those of the author(s) only and do not necessarily reflect those of the European Union. Neither the European Union nor the granting authority can be held responsible for them.

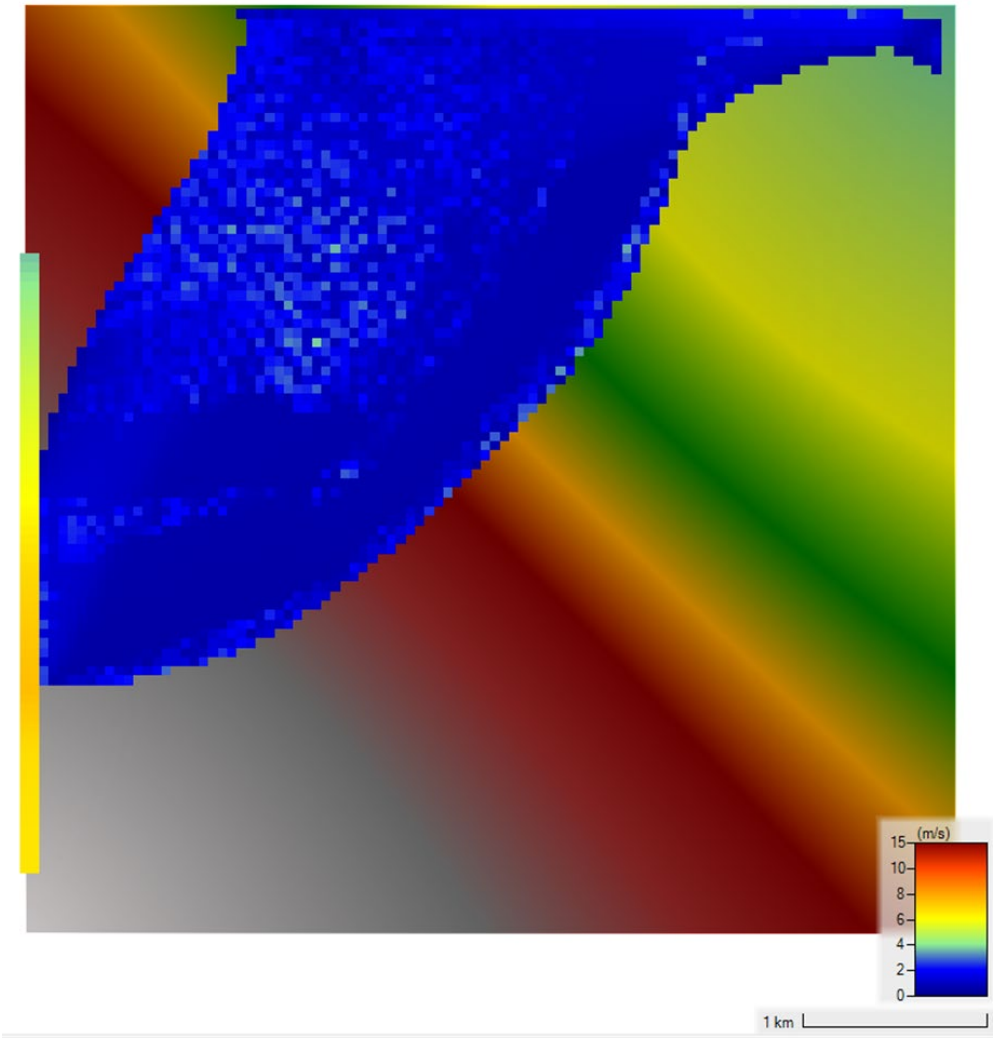

Figure 3.7. GeoTIFF map with simulated water velocity in the floodplain. In this case flow velocities are less than 2m/s in all the flooded area. The map shows the DTM in background.

Funded by the European Union. Views and opinions expressed are however those of the author(s) only and do not necessarily reflect those of the European Union. Neither the European Union nor the granting authority can be held responsible for them.

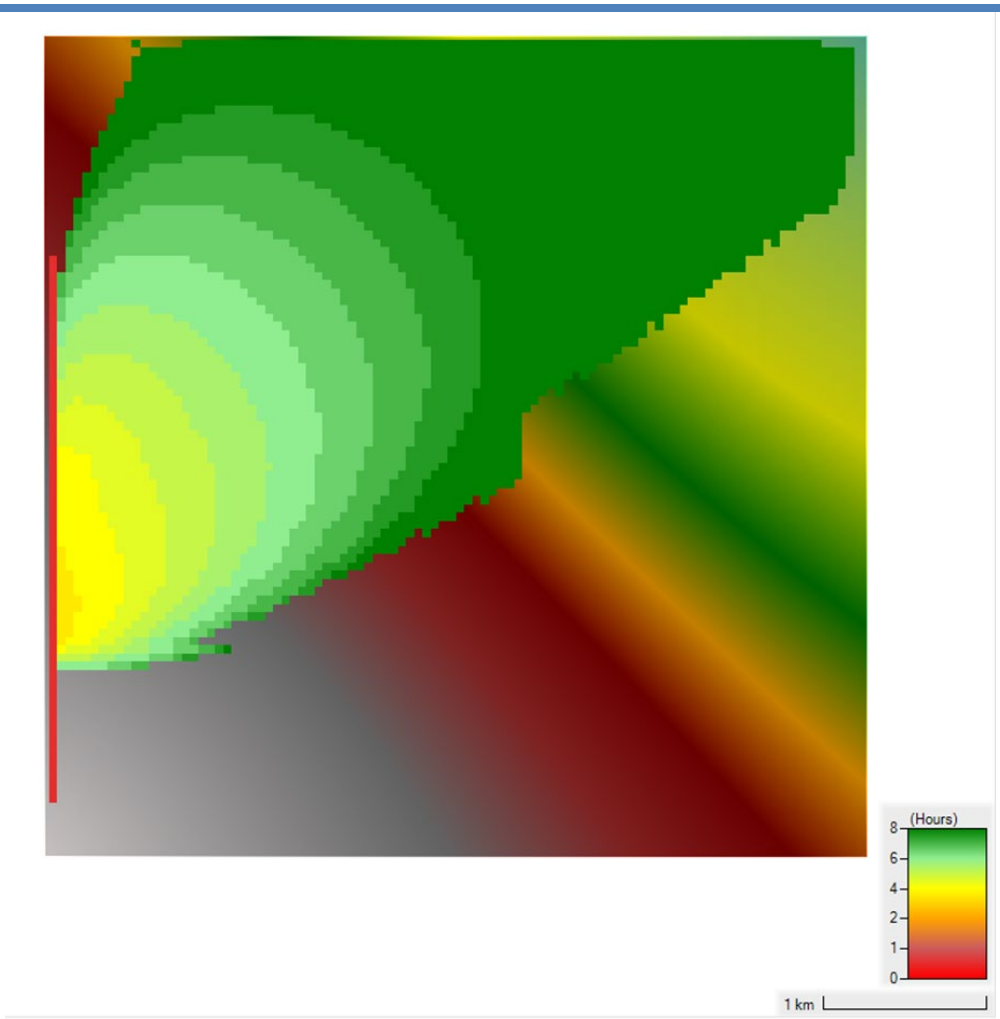

Figure 3.8. Example of GeoTIFF map with simulated arrival time (hours). The map shows the DTM in background.

Finally, the volume of the floods on the floodplain is reported in the following table. These volumes can provide an estimation of the water depth when barriers or constraints make a limitation to the expansion of the flood.

Funded by the European Union. Views and opinions expressed are however those of the author(s) only and do not necessarily reflect those of the European Union. Neither the European Union nor the granting authority can be held responsible for them.

Table 3.2. Examples of estimated flooded volumes for different simulated scenarios. In this format, the comma is used to separate thousands.

PLAN	volume esondato (mc)
A2-MMM-TR010	5,500
A2-MMM-TR030	24,300
A2-MMM-TR100	60,000
A2-MMM-TR200	93,300
A2-MHH-TR010	5,500
A2-MHH-TR030	24,300
A2-MHH-TR100	60,000
A2-MHH-TR200	93,400
A2-LLL-TR010	0
A2-LLL-TR030	1,750
A2-LLL-TR100	33,800
A2-LLL-TR200	86,700
A10-MMM-TR010	0
A10-MMM-TR030	0
A10-MMM-TR100	90,000
A10-MMM-TR200	300,000
A10-MHH-TR010	0
A10-MHH-TR030	0
A10-MHH-TR100	91,000
A10-MHH-TR200	350,000
A10-LLL-TR010	8,000
A10-LLL-TR030	59,000
A10-LLL-TR100	170,000
A10-LLL-TR200	279,000
A100-MMM-TR010	0
A100-MMM-TR030	119,000
A100-MMM-TR100	885,000
A100-MMM-TR200	1,641,000
A100-MHH-TR010	0
A100-MHH-TR030	119,000
A100-MHH-TR100	884,000
A100-MHH-TR200	1,640,000
A100-LLL-TR010	8,000
A100-LLL-TR030	431,000
A100-LLL-TR100	2,000,000
A100-LLL-TR200	3,600,000
A1000-MMM-TR010	620,000
A1000-MMM-TR030	5,000,000
A1000-MMM-TR100	17,400,000
A1000-MMM-TR200	27,700,000
A1000-MHH-TR010	620,000
A1000-MHH-TR030	4,900,000
A1000-MHH-TR100	17,400,000
A1000-MHH-TR200	27,600,000
A1000-LLL-TR010	0
A1000-LLL-TR030	550,000
A1000-LLL-TR100	4,800,000
A1000-LLL-TR200	9,800,000
A10000-MMM-TR010	3,000,000
A10000-MMM-TR030	8,900,000
A10000-MMM-TR100	28,000,000
A10000-MMM-TR200	49,000,000
A10000-MHH-TR010	3,000,000
A10000-MHH-TR030	8,800,000
A10000-MHH-TR100	26,000,000
A10000-MHH-TR200	53,000,000
A10000-LLL-TR010	0
A10000-LLL-TR030	3,200,000
A10000-LLL-TR100	20,600,000
A10000-LLL-TR200	37,000,000

Funded by the European Union. Views and opinions expressed are however those of the author(s) only and do not necessarily reflect those of the European Union. Neither the European Union nor the granting authority can be held responsible for them.

3.2. CLASS OF DAMAGE

Flood events affect territories in different ways depending on what elements are exposed and how vulnerable they are. For this reason, the classification of damage potential is a key step in flood risk assessment and territorial planning. In accordance with the EU Floods Directive (2007/60/EC) and its Italian implementation (Legislative Decree 49/2010), four damage classes were established to categorize areas based on the type, value, and vulnerability of the exposed elements.

These classes—D1 (Low), D2 (Moderate), D3 (Medium), and D4 (High)—reflect a progressively increasing level of potential consequences in the event of flooding. The classification is primarily derived from land use, and considers a variety of spatial features, including residential, commercial, agricultural, environmental, and infrastructural components.

- D1 – Low Damage Class
  This class includes areas with limited or negligible human presence and low economic value. Typical examples include natural areas, forests, unbuildable agricultural zones, and unbuilt public land. In these areas, the impact of flooding is minimal and rarely results in significant damage or disruption.
- D2 – Moderate Damage Class
  Areas in this class host non-strategic infrastructure, buffer zones, and green public or private spaces, such as parks or protected landscapes. Although development is limited, flooding can still cause moderate disruption to public amenities, ecosystems, or secondary services.
- D3 – Medium Damage Class
  This class involves zones with functional infrastructure and productive land that are not densely built-up but are nonetheless important. These may include railways, utility lines (lifelines), land with development potential, and industrial utility areas such as waste treatment or quarry zones. Flooding in these areas could lead to economic losses, environmental concerns, and disruption of regional services.
- D4 – High Damage Class
  The highest damage class is assigned to urban areas, historical settlements, and strategic or densely built environments. It includes critical infrastructure, residential and commercial zones, public services, hazardous waste areas, and tourism facilities (e.g., hotels and campsites). Here, flood events here can lead to major economic damage, human safety risks, and long-term disruptions to key services.

The classification of damage plays a foundational role in determining the flood risk. When combined with hazard levels, it enables the definition of hydraulic risk classes. It is also an essential tool for:

- Structuring risk prioritization in civil protection and emergency planning;
- Supporting flood risk mapping and communication with stakeholders;
- Guiding land-use planning to prevent or reduce exposure;
- Facilitating the allocation of public funds for risk mitigation strategies.

Funded by the European Union. Views and opinions expressed are however those of the author(s) only and do not necessarily reflect those of the European Union. Neither the European Union nor the granting authority can be held responsible for them.

Table 3.2 provides a summary of the defining characteristics of each damage class.

Table 3.2. Definition of damage classes.

Code	Class of demage	Description of land use
D1	Low	Woodland area
		Non-buildable agricultural area
		Unbuilt or unbuildable public land
D2	Moderate	Public infrastructure (non-strategic municipal or consortium roads)
		Environmental protection area, buffer zones, private green areas
		Parks, unbuilt public green areas
D3	Medium	Railways
		Lifelines: power lines, pipelines, aqueducts
		General agricultural area (with building potential)
		Area for technological plants, municipal waste landfills; quarry zones
D4	High	Urban centers
		Minor rural centers of particular value
		Completion areas
		Expansion areas
		Artisan, industrial, commercial areas
		Public services mainly with buildings
		Public infrastructures (e.g., main and strategic roads and services)
		Area for disposal of hazardous or special waste
		Hotel area
		Area for campsites and tourist villages

3.3. HYDRAULIC HAZARD

The hydraulic hazard expresses the likelihood and physical intensity of a flood event, regardless of what might be exposed. It focuses on measurable hydrological characteristics such as flood depth, flow velocity, duration, and most importantly, return period (Tr)—which indicates how frequently a flood of a given magnitude is statistically expected to occur.
In line with the EU Floods Directive, hydraulic hazard is classified into three levels:

- P3 – High Hazard
  This level refers to frequent and intense flood events, typically associated with a return period of 30 years or less (Tr ≤ 30 years). These floods may occur more than once in a generation and are considered a serious threat to safety, infrastructure, and property.
- P2 – Medium Hazard
  This class includes moderate-probability flood events, with a return period between 30 and 200 years (30 < Tr ≤ 200 years). These are less frequent than high-hazard events but still present significant risks, especially in populated or economically active areas.
- P1 – Low Hazard
  This level represents rare flood events, with a return period greater than 200 years (Tr > 200 years). Although these floods are infrequent, they can still be dangerous—particularly

Funded by the European Union. Views and opinions expressed are however those of the author(s) only and do not necessarily reflect those of the European Union. Neither the European Union nor the granting authority can be held responsible for them.

in cases of extreme weather conditions, climate change, or infrastructure failure.

The classification of hydraulic hazard is essential for:

- Delimiting flood hazard zones for maps and regulatory purposes;
- Designing preventive and mitigation measures proportional to the risk;
- Informing emergency response strategies and civil protection planning.

Table 3.3 summarizes the criteria associated with each hydraulic hazard class.

Table 3.3. Definition of hydraulic hazard classes.

Code	Class of hydraulic hazard	Description
P3	High	Flood for $Tr \leq 30$ years
P2	Medium	Flood for $30 \text{ years} < Tr \leq 200$ years
P1	Low	Flood for $Tr > 200$ years

3.4. HYDRAULIC RISK ASSESSMENT

Hydraulic risk is the result of combining the likelihood of a flood event (hazard) with the potential severity of its consequences (damage). It reflects the probability that a flood will occur and the extent of its impact.
In line with the EU Floods Directive (2007/60/EC), hydraulic risk is herein assessed by combining:

- Hydraulic Hazard Classes (P1–P3);
- Damage Classes (D1–D4).

This two-dimensional assessment results in the identification of four hydraulic risk classes, which represent an increasing level of threat to people, property, infrastructure, and the environment (Table 4):

- R1 – Low or No Risk:
  Damage is minimal or non-existent. Floods may occur but have negligible impact due to the nature of the exposed area and the limited hazard.
- R2 – Medium Risk:

Funded by the European Union. Views and opinions expressed are however those of the author(s) only and do not necessarily reflect those of the European Union. Neither the European Union nor the granting authority can be held responsible for them.

Moderate consequences are expected. Floods may affect economic activities or services, but do not generally pose a threat to life or strategic infrastructure.

- R3 – High Risk:
  Significant adverse effects are possible, including threats to public safety, economic productivity, and key infrastructure. Recovery efforts may be substantial.
- R4 – Very High Risk:
  These scenarios include potential loss of life, severe injuries, and destruction of critical assets or irreplaceable heritage sites. Immediate action is required to reduce or avoid exposure.

This classification supports the creation of detailed risk maps, the formulation of land-use regulations, and the prioritization of structural and non-structural mitigation measures.
The assessment can be done using a risk matrix, where:

- The vertical axis corresponds to the class of damage (D1–D4), and
- The horizontal axis corresponds to the hydraulic hazard class (P1–P3).

This matrix offers a clear and consistent framework to:

- Evaluate and communicate levels of flood risk in a standardized way;
- Support zoning, urban development controls, and building regulations;
- Enable strategic planning for emergency services and public authorities;
- Guide investment decisions in flood protection infrastructure and land management.

Table 3.4 outlines the characteristics of each hydraulic risk class, whereas Table 3.5 illustrates the matrix used to determine risk based on hazard and damage inputs.

Table 3.4. Definition of hydraulic risk classes.

Code	Class of hydraulic risk	Description
R4	Very High Risk	Possible loss of human life and serious injuries, major damage to buildings, infrastructure, and environmental heritage, and destruction of socio-economic activities.
R3	High Risk	Possible threats to personal safety, major functional damage to buildings and infrastructure resulting in their unavailability, interruption of socio-economic activities, and damage to environmental heritage.
R2	Medium Risk	Possible minor damage to buildings, infrastructure, and environmental heritage, without compromising people's safety, building usability, or economic activity functionality.
R1	Low or No Risk	Social, economic, and environmental damage is negligible or non-existent.

Funded by the European Union. Views and opinions expressed are however those of the author(s) only and do not necessarily reflect those of the European Union. Neither the European Union nor the granting authority can be held responsible for them.

Table 3.5. Hydraulic risk matrix.

Class of hydraulic risk		Class of hazard		
		P3	P2	P1
Class of damage	D4	R4	R3	R2
	D3	R3	R3	R1
	D2	R2	R2	R1
	D1	R1	R1	R1

Funded by the European Union. Views and opinions expressed are however those of the author(s) only and do not necessarily reflect those of the European Union. Neither the European Union nor the granting authority can be held responsible for them.

4. RISK PERCEPTION OF REFERENCE ELEMENTS (PEOPLE)

Floods and Landslides: An Introduction to the Psychological Consequences and Risk Perception

Floods and landslides could have adverse impacts on the mental health of the affected populations (see Deliverable D3.1, section people) in terms of increasing levels of Post-traumatic Stress Disorder (PTSD), depression, and anxiety symptomatology (Kumar, 2023; Walinski et al., 2023; Kabunga, 2022; Parel & Balamurugan, 2021; Fernandez et al., 2015). These psychological consequences can negatively affect people's lives, leading to significant difficulties in social and relational skills, work and school performance, reduced quality of life, and physical health issues (APA, 2022). The literature also showed that certain groups of the population (children, the elderly, and subjects with previous traumas, and special needs could be more vulnerable to the onset of psychological consequences (Cianconi et al., 2020; Sharpe & Davidson, 2022; White et al., 2023; Medved et al., 2022; Maltais, 2019; Han, 2017; Walker et al., 2015; Aldrich & Benson, 2008; Peek, 2008; Miller & Arquilla, 2008). The increased vulnerability to adverse psychological consequences of the population affected by floods and landslides could also be influenced by other risk and protective factors (i.e., socio-demographic, pre-traumatic, peri-traumatic, and post-traumatic factors) described in deliverable D3.1. Based on the indications of the Process Oriented Model (Cummings, Davies, & Campbell, 2000; Di Blasio, 2005), we classified the most significant PTSD/anxiety/depression risk and protective factors (see Section 1 of the Deliverable D3.1) as distal and proximal factors. The term “Distal” is used because these factors are supposed to affect adjustment/maladjustment indirectly and can be thought of as a humus on which more proximate events and factors build their influence. Proximal factors include both risk and protective factors: risk factors exacerbate vulnerability induced by distal factors, increasing the probability that the situation evolves into adverse conditions. Conversely, protective factors are proximal resources that may buffer the negative impact of distal and proximal risk factors.

Another line of research outlines the significant *role of flood and landslide risk perception* (see Deliverable D3.1, section people). Risk perception refers to subjective assessments of the perceived probability regarding the occurrence and severity of a hazard event, which influence the preparedness, response, and mitigation behaviors that precede, accompany, and follow the event (Bradford et al., 2012; Lechowska, 2022). Therefore, how people perceive and understand risk can affect how they prepare and respond to natural hazards (Lechowska, 2022; Bradford et al., 2012). Adequate risk perception in people appears to be linked to good risk awareness and prior knowledge of the appropriate protective behavior to adopt in case of an emergency (Marincioni, 2020). It could thus support effective emergency response and management because it is linked to early recognition of real risk and subsequent timely implementation of the correct protective behaviors, increasing self-efficacy and personal safety.

Funded by the European Union. Views and opinions expressed are however those of the author(s) only and do not necessarily reflect those of the European Union. Neither the European Union nor the granting authority can be held responsible for them.

Conversely, inadequate risk perception, both in terms of underestimation and overestimation, can interfere with effective emergency response and management (Lechowska, 2018), contributing to amplifying the level of personal exposure to hazards (Wachinger et al., 2010) and consequent possible repercussions on psychophysical vulnerability.
Specifically, people with low risk perception may not have a good awareness of hazards and knowledge of protective behaviors to implement. Therefore, in case of emergency, they may underestimate hazards, engage in reckless and risky behaviors, or delay the implementation of protective behaviors (Ding et al., 2020).
On the other hand, people with high risk perception are generally more aware of risks and knowledgeable about protective behaviors to adopt in case of emergency (Ding et al., 2020). However, they may be more vulnerable to intense and dysfunctional emotional reactions (Zhao et al., 2023), such as high anxiety and fear, panic, or impulsive behaviors. In emergency settings, such emotional reactions may hinder the ability to rationally assess the situation and make effective decisions, leading to the enactment of hasty, counterproductive, and potentially harmful and dangerous choices.

In this direction, considering the quality of risk perception could be a significant component in developing an effective preventive preparedness system and strategic risk communication practices (Ali et al., 2022; Paek & Hove, 2017) (see Deliverable D3.3). Literature (see deliverable D3.1) outlined how the quality of risk perception could be affected by some significant factors and conditions such as sociodemographic and personality factors, information and knowledge, awareness and worry, and the direct experience of a hazard (see figure 4.1). These elements should be considered to assess the quality of risk perceptions.

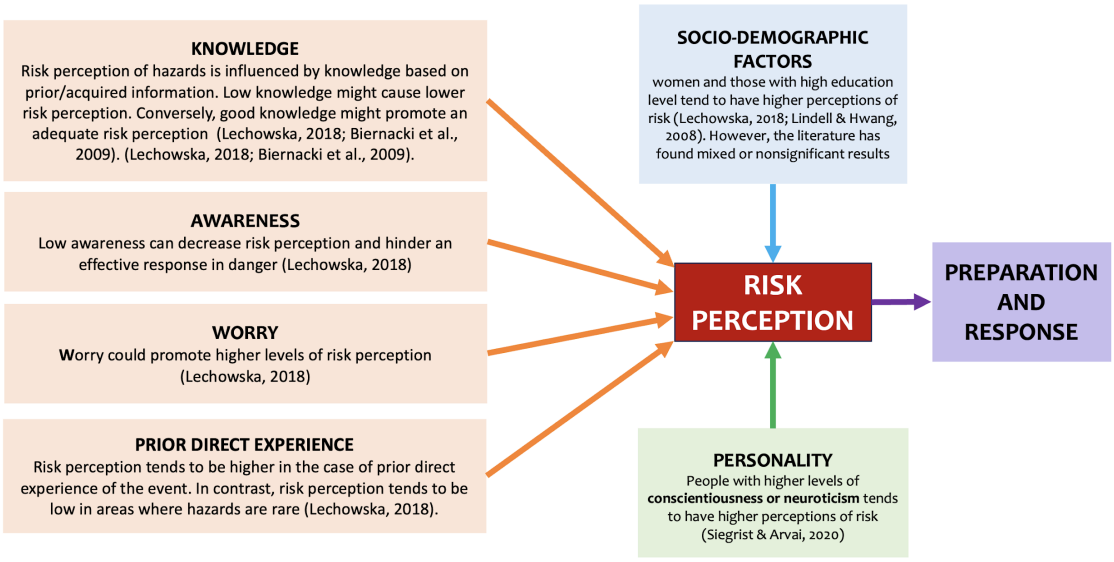

Figure 4.1: Factors that may influence risk perception

Funded by the European Union. Views and opinions expressed are however those of the author(s) only and do not necessarily reflect those of the European Union. Neither the European Union nor the granting authority can be held responsible for them.

PEOPLE: **Identifying individuals at risk of psychological consequences and assessing the quality of Risk Perception in the case of floods and landslides.**

Aims:
Based on the above-cited literature, the psychological section of the SAFE-LAND project had the twofold objective of investigating the factors that may influence: a) the risk of psychological vulnerability in case of floods and landslides; b) the quality of risk floods and landslides perception (in terms of low risk perception; adequate risk perception and high risk perception).

Procedures:
A preliminary study (pre-test) was conducted on a non-representative reference convenience sample (reference people) to collect preliminary data on the research protocol.
Specifically, during this pre-test phase, a web survey was created (on the Qualtrics platform) and distributed to reference people through a QR-CODE/link via email and social media sites of the research staff.
More specifically, participants accessed through a QR code or link the web survey which described the research protocol's objectives and included a series of questionnaires listed in Table 4.1. Participation in the survey was voluntary, and subjects had to give their informed consent to participate and to data treatment before answering the questions. The survey took approximately 20 minutes to complete. In treating the participants, we followed APA guidelines, the 1964 Helsinki Declaration, and its later amendments or comparable ethical standards. The Ethical Committee of e-Campus University also approved the research protocol (No. 6/2024).

Table 4.1: The Research Protocol

RESEARCH PROTOCOL	
1. Socio-demographic inventory	Socio-demographic data
2. Risk perception of floods and landslide	Knowledge, awareness, worry, and prior direct experience about floods and landslides
3. Climate Change Worry Scale (CCWS, Stewart, 2021)	Worry about climate change
4. Multidimensional Scale of Perceived Social Support (MSPSS, Zimet et al., 1988)	Perceived social support
5. World Health Organization - Five Well-Being (WHO-5, WHO, 1998)	Psychological well-being
6. Psychological general well-being (PGWB, Dupuy, 1984)	Psychological well-being
7. Big Five Inventory 10 (BFI-10, Rammstedt, & John, 2007)	Personality
8. Brief Cope (Carver, 1997)	Coping strategies
9. Primary Care PTSD Screen for DSM-5 (PC-PTSD-5, Prins et al., 2016)	Vulnerability to PTSD symptoms

Funded by the European Union. Views and opinions expressed are however those of the author(s) only and do not necessarily reflect those of the European Union. Neither the European Union nor the granting authority can be held responsible for them.

A non-representative convenience sample of 124 participants (79.5% females) aged between 20 and 69 (mean value, M = 36.7; standard deviation, SD = 12.4) participated in the web survey. A summary of the participants' demographic characteristics is in Table 4.2. A significant number of participants were married or cohabiting (63%) and well educated (60% with more than a high school degree), and with a profession in scientific, technical, and human fields (42%).
It is worth noting the higher level of female participation compared to male participation in the web survey. However, this is a common finding in the literature and can be attributed to differences in the way males and females make decisions and value actions in the online environment (Smith, 2008). The social exchange theory is based on the idea that people make decisions about exchanges based on their separate self-concepts (England, 1989; Smith, 2008). Separative characteristics are more likely to be valued by males. At the same time, females are more likely to value characteristics that are more consistent with connective selves, such as empathy or emotional closeness. Therefore, if becoming a survey respondent is more likely to be seen as something that connective selves do more often than separative selves, or is seen as more valuable by people who have characteristics of connective selves, then we would expect to see a higher survey response rate from females than from males (Smith, 2008).

The higher female response rate certainly represent a limitation of this pre-test. However, the other socio-demographic variables in the pre-test were found to have a good level of representation.
The questionnaire continues to be sent to the sample population, and the database with the questionnaire responses is continuously updated, in order to build a larger and more representative sample.

Funded by the European Union. Views and opinions expressed are however those of the author(s) only and do not necessarily reflect those of the European Union. Neither the European Union nor the granting authority can be held responsible for them.

Table 4.2: Demographic characteristics of the sample

		N	%
Education	High School Degree or less	50	40,3
	More than High School Degree	74	59,7
Profession	Students	35	28%
	Simple profession; Unemployed	5	4%
	Skilled Workers	4	3,00%
	Service and Sales Occupation	25	23%
	Professional in Scientific, Tecnical and Human Fields	55	42%
Relational Status	Single	36	29%
	Childless Couples	41	32%
	Families with Children	38	31%
	Single Parents	8	7%
	Widowed	1	1%
Income	17,000 Euro or less	76	60%
	From 17,000 to 35,000 euro	18	15%
	More than 35,000 Euro	30	25%

Results: Identification of individuals at risk of vulnerability to adverse psychological consequences

To detect the individuals at risk of adverse psychological consequences, we considered a series of variables classified as resources, distal risk factors, and proximal risk and protective factors (see Deliverable D3.1, pages 19-20). Specifically, based on the indications of the literature, we considered a series of socio-demographic factors (i.e., gender, age, education, and occupation); and individual and relational pre-traumatic factors (i.e., prior traumatic events, personal and family special needs, coping strategies, social support) that we categorized in terms of resources, distal risk factors, and proximal risk and protective factors (see Table 4.3).

Co-funded by the European Union
Funded by the European Union. Views and opinions expressed are however those of the author(s) only and do not necessarily reflect those of the European Union. Neither the European Union nor the granting authority can be held responsible for them.

Table 4.3: Risk and protective factors considered to assess the levels of vulnerability to psychological risk

IDENTIFICATION OF INDIVIDUALS AT RISK OF VULNERABILITY TO ADVERSE PSYCHOLOGICAL CONSEQUENCES				
RESOURCES (-0,5)	**PROXIMAL PROTECTIVE FACTORS (-1)**	**DISTAL RISK FACTORS (+0,5)**	**PROXIMAL RISK FACTORS (+1)**	**LEVELS OF VULNERABILITY TO PSYCHOLOGICAL RISK**
High education level Employment	Positive coping strategies, Social support, Psychological well-being	Female gender, Low education level Unemployment Low Income Prior traumatic events Older age	Personal and family history of special needs Negative coping strategies Low psychological well-being Low social support	**0 – NO RISK** (only resources or proximal protective factors, eventually 1 distal risk factor) **1 – LOW RISK** (prevalence of resources or proximal protective factors) **2 – RISK** (compresence of protective and risk factors) **3 – HIGH RISK** (prevalence of distal and proximal risk factors)

First, we categorized each considered variable (for example: gender, age, socio-economic status, previous traumatic events, special needs, psychological well-being, coping strategies, and social support) in terms of resources, distal, and proximal factors. Then we assigned a specific score (see Table 3) to **resources** (Score = **- 0,5**), **distal risk factor** (Score **0,5**), **proximal risk** (Score = **1**), or proximal **protective factors (**Score = **-1**). Second, we calculated each subject's total vulnerability score (ranging from -5.5 to 6; M = -1.1; DS = 2.5) by considering the scores of each variable. Third, we performed a K-means statistical analysis to identify four groups of individuals with distinct risk levels of negative psychological consequences. **The four levels of vulnerability include no risk, low risk, presence of risk, and high risk of psychological vulnerability** (see Table 4.3).

Results for the Assessment of the Risk of Vulnerability to Adverse Psychological Consequences

The results indicated that 50 participants (40,3%) showed no risk of adverse psychological consequences; 38 (30,6%) showed a low risk of adverse psychological consequences; 33 (26,6%) showed a risk of adverse psychological consequences, and finally 3 (2,4%) showed a high risk of adverse psychological consequences (Figure 4.2)

Funded by the European Union. Views and opinions expressed are however those of the author(s) only and do not necessarily reflect those of the European Union. Neither the European Union nor the granting authority can be held responsible for them.

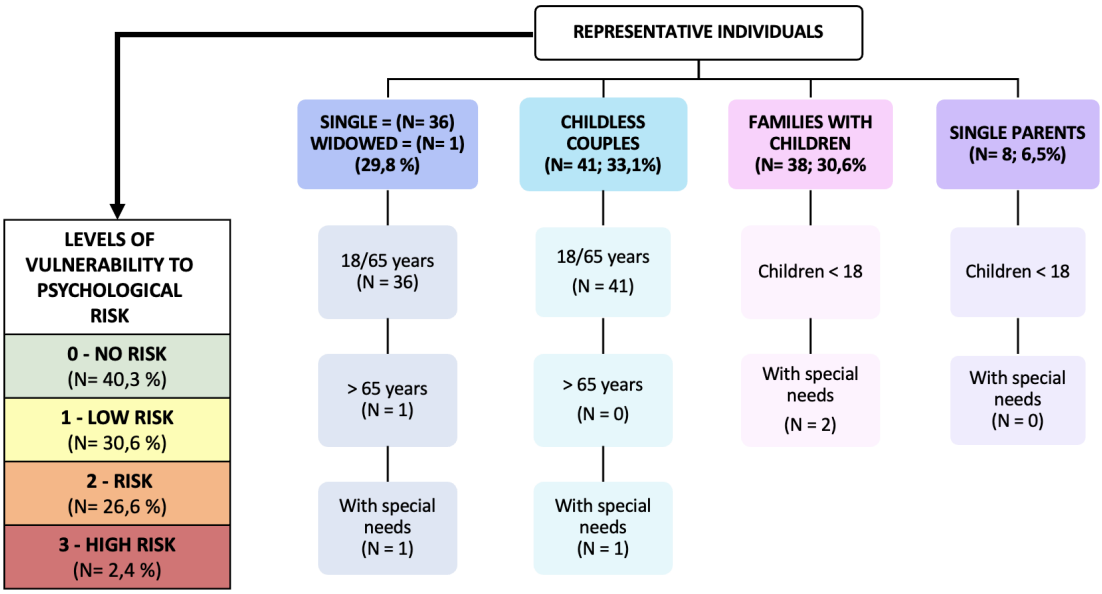

Figure 4.2: Participants' psychological risk levels.

Results: Assessing the Quality of Risk Perception

To detect each participant's quality of risk perception for floods and landslides, we considered a series of variables following the indications of the literature (see Deliverable D3.1). We assessed variables that affect risk perception for floods and landslides separately. Through a series of questionnaires, we considered the participants' personality characteristics and the level of knowledge, awareness, worry, and prior direct experience of floods and landslides. In Tables 4.4 and 4.5, we reported, in detail, the variables considered to assess the participants' risk perception and the three degrees of risk perception.

Table 4.4: Factors that influence risk perception and degree of risk perception

ASSESSMENT OF THE QUALITY OF RISK PERCEPTION					
Knowledge	Awareness	Worry	Prior direct experience of floods or landslides	Personality	DEGREE OF RISK PERCEPTION
					0 – LOW RISK PERCEPTION
					1 – ADEQUATE RISK PERCEPTION
					2 – HIGH RISK PERCEPTION

Co-funded by the European Union
Funded by the European Union. Views and opinions expressed are however those of the author(s) only and do not necessarily reflect those of the European Union. Neither the European Union nor the granting authority can be held responsible for them.

Table 4.5: The assessment of risk perception

Factors affecting risk perception	VARIABLES AND FINAL SCORE
KNOWLEDGE Good knowledge might promote an adequate risk perception (Lechowska, 2018; Biernacki et al., 2009).	**Knowledge was assessed through the following statements about:** 1. Knowledge of Previous local floods or landslides (Yes/No) 2. Knowledge of response behaviours and emergency management in case of floods or landslides (e.g., protective behaviors, warning systems, risk/safe areas, etc.) (Selection of known options) 3. Keep informed about flood, landslide, and weather warnings (from 0= not informed to 3= very informed) 4. Level of knowledge on how to protect oneself/respond in case of flood/flood, or landslide (from 0= no knowledge to 3 = a lot of knowledge) Based on these four items, we created a final unique variable titled **Knowledge**. For this variable, we assigned to each participant a score of -1, in case of low knowledge and a score of 0 in case of adequate or high knowledge.
AWARENESS Low awareness can decrease risk perception and hinder an effective response in danger (Lechowska, 2018).	**Awareness was assessed using the following statements about:** 1. Awareness of living in a flood/landslide risk area *(0 = No, 1 = don't know, 2 = Yes)* 2. Awareness of areas in the city most at risk of flooding or landslides (from 3= the city has the same risk everywhere to 0= don't know) 3. Awareness of the causes of flooding and landslides (Selection of known options) Based on these three items, we created a final unique variable titled **Awareness.** For this variable, we assigned to each participant a score of -1, in case of low awareness and a score of 0 in case of adequate awareness and a score of 1 for high awareness
WORRY Worry could promote higher levels of risk perception (Lechowska, 2018)	**Worry was assessed using the following statements about:** 1. Emotional response experienced in the past or anticipated in the future if a flood or landslide were to occur (from calm to terror) 2. Level of worry in response to a flood or landslide warning for the following day *(0 = Not worried at all to 3 = Extremely worried)* Based on these two items, we created a final unique variable titled **Worry** For this variable, we assigned to each participant a score of -1, in case of low worry and a score of 0 in case of adequate worry and a score of 1 in case of high worry
PRIOR DIRECT EXPERIENCE Risk perception tends to be higher in case of prior direct experience of the event (Lechowska, 2018).	Past Experience was assessed the following statement about: 1. Type of past experience with floods or landslides *(Options: Direct personal experience, Direct experience of a friend or relative, Information from news or other media, None of the above)* Based on this item, we created a final unique variable titled **Experience.** For this variable, we assigned to each participant a score of -1, in case of absent experience and a score of 0 in case of indirect experience and a score of 1 in case of direct experience
PERSONALITY People with higher levels of conscientiousness or neuroticism tend to have a higher perception of risk (Siegrist & Arvai, 2020).	Personality was assessed through the Big Five Inventory-10 (BFI-10, Rammstedt & John, 2007). We considered the two variables conscientiousness and neuroticism and we created a final unique variable titled **Personality.** For this variable, we assigned to each participant a score of -1, in case of low neuroticism and conscientiousness and a score of 0 in case of adequate neuroticism and conscientiousness and a score of 1 in case of high conscientiousness and neuroticism.

Funded by the European Union. Views and opinions expressed are however those of the author(s) only and do not necessarily reflect those of the European Union. Neither the European Union nor the granting authority can be held responsible for them.

To assess the quality of risk perception for both floods and landslides, we considered the five variables (knowledge, awareness, worry, prior direct experience, and personality) and assigned a score to each (See Table 4.5). Then, we calculated a total score for each participant about the risk perception of floods (scores from -4 to 4) and landslides (scores from -3 to 5). Then, we performed a K-means statistical analysis to identify three groups of individuals with distinct levels of quality of risk perception for floods and landslides: low, adequate, and high risk perception.

Results for the assessment of flood and landslide risk perception

The results regarding flood risk perception showed that 13 participants (10.5%) had a low risk perception; 76 (61,3%) had a correct risk perception, and finally, 35 (28,2%) had a high risk perception (Figure 4.3).

Results regarding landslide risk perception showed that 24 participants (19.4%) had a low risk perception; 78 (62,9%) had a correct risk perception, and finally, 22 (17.7%) had a high risk perception (Figure 4.3).

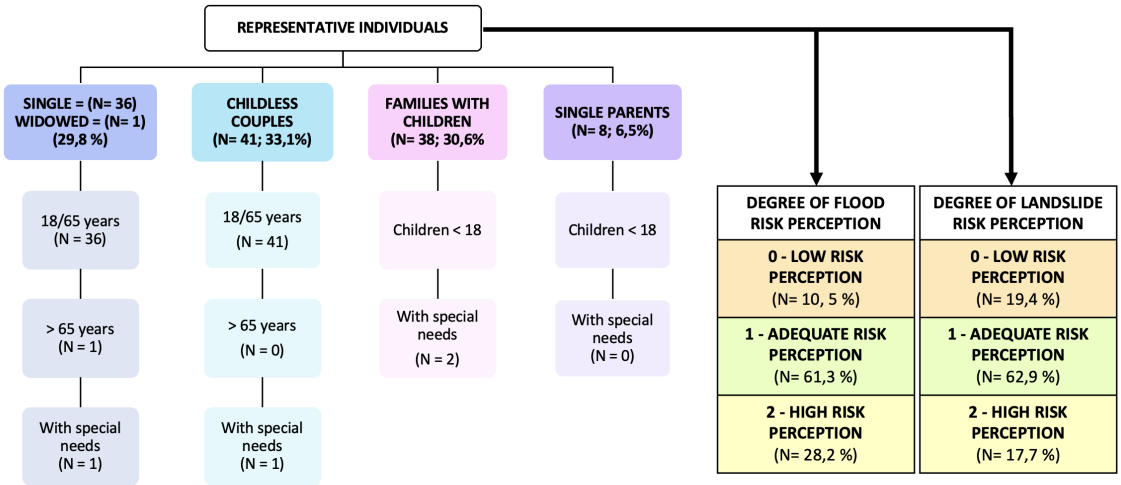

Figure 4.3: Participants' degree of risk perception

Co-funded by the European Union

Funded by the European Union. Views and opinions expressed are however those of the author(s) only and do not necessarily reflect those of the European Union. Neither the European Union nor the granting authority can be held responsible for them.

In summary, the psychological part of the SAFE-LAND project aimed to create a system capable of early identification of vulnerability to psychological risk and to assess the quality of risk perception, in case of floods or landslides (see Figure 4.4).

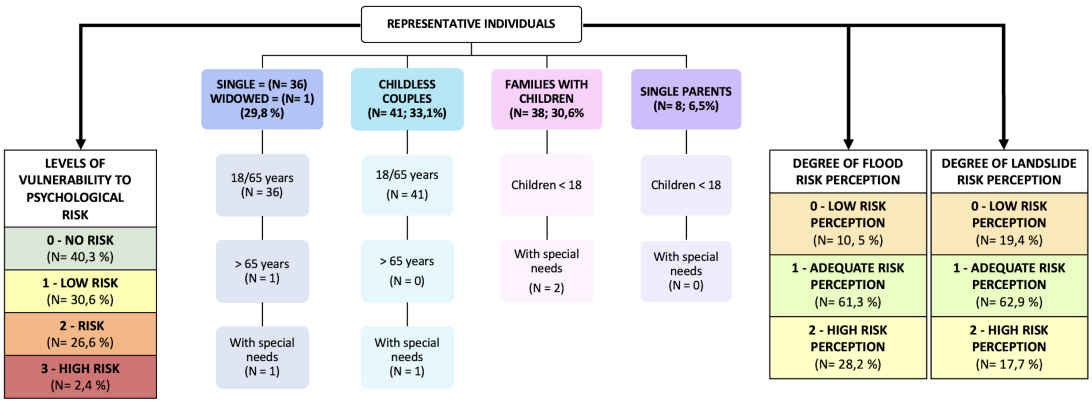

Figure 4.4: Results About the Population's Vulnerability to Psychological Risk, And Quality Of Floods/Landslides Risk Perception

Regarding the vulnerability to psychological risk, based on the indications of the literature, we outlined that some socio-demographic and pre-traumatic variables can significantly influence an individual's vulnerability to psychological risk. Specifically, a series of individual and relational variables (distal and proximal risk factors) could amplify vulnerability to psychological risk or protect psychological well-being (proximal resources and protective factors). These factors could constitute a risk or protective humus that leads individuals to show different baseline levels of vulnerability to psychological consequences even before a flood or landslide event occurs. Understanding and assessing these preexisting factors could provide essential insights into an individual's vulnerability to psychological risk, as it could worsen and become chronic after the emergency, especially in the presence of severe peri- and post-traumatic factors. Therefore, identifying individuals' vulnerabilities and strengthening and supporting their protective adaptive resources and functioning at the individual and relational levels could constitute effective preventive interventions. Similarly, it is significant to consider the quality of the population's perception of risk in floods and landslides because it is relevant to people's preparation and appropriate responses in case of emergency (see Deliverable D3.3). For example, an adequate perception of risk could support effective emergency response and management because it is connected to the early recognition of the real risk and the subsequent timely implementation of the correct protective behaviors (Marincioni, 2020). Conversely, inadequate risk perception (low and high), can interfere with effective emergency response and management (Lechowska, 2018), contributing to amplifying the level of personal exposure to hazards (Wachinger et al., 2010) and consequent possible repercussions on psychophysical vulnerability.

Funded by the European Union. Views and opinions expressed are however those of the author(s) only and do not necessarily reflect those of the European Union. Neither the European Union nor the granting authority can be held responsible for them.

In Deliverable D3.3, some intervention guidelines based on four cyclical phases of the emergency management system (people's hazard preventive preparedness, risk communication, response to event, and post-event recovery) will be described. Specifically, these four phases will be implemented by considering both the quality of risk perception and the psychological vulnerability of individuals in case of floods and landslides (Figure 4.5).

Guidelines will be proposed to improve the emergency management system through the:

1- **Promotion of effective preventive preparation and risk communication that support adequate knowledge and awareness of risks and consequent functional and protective response in the event of a flood/landslide emergency.**

2- **Promotion of early identification of the subjects most vulnerable to adverse psychological consequences in the event of floods/landslides in the post-event recovery phase.**

Figure 5: Phases of the Guidelines to support an effective emergency management system through the promotion of adequate risk perception and consideration of psychological vulnerability in the case of floods and landslides

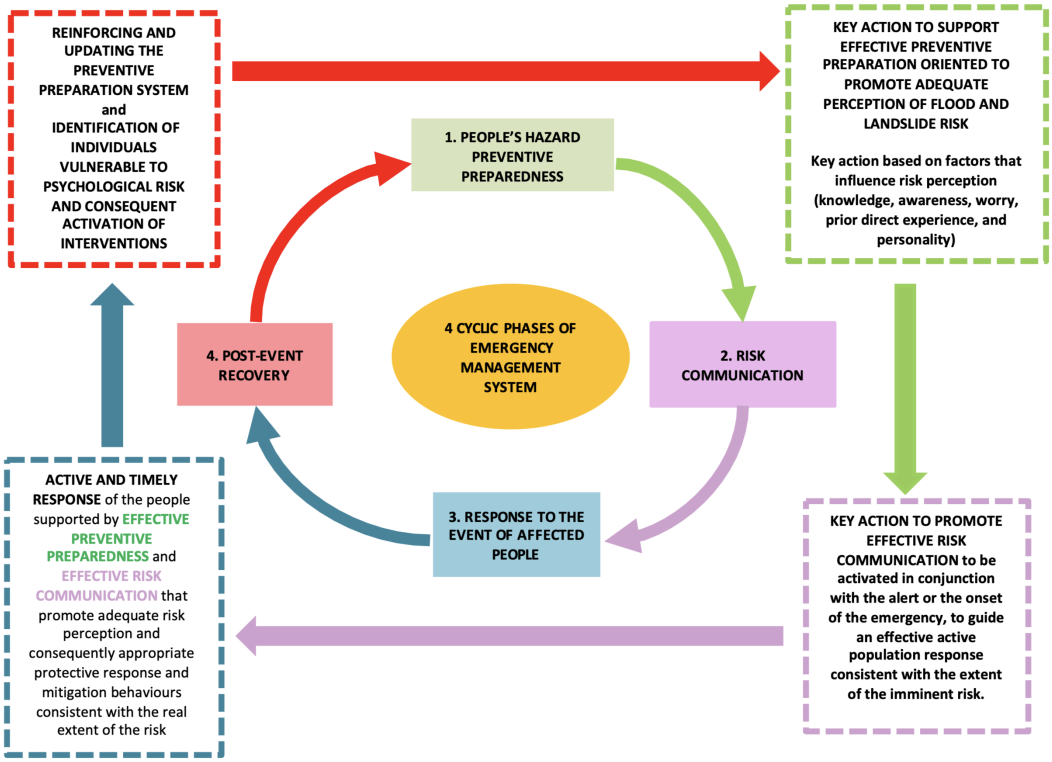

Funded by the European Union. Views and opinions expressed are however those of the author(s) only and do not necessarily reflect those of the European Union. Neither the European Union nor the granting authority can be held responsible for them.

5. REFERENCES

Ali, A., Rana, I. A., Ali, A., & Najam, F. A. (2022). Flood risk perception and communication: The role of hazard proximity. Journal of Environmental Management, 316, 115309.

Aldrich, N., & Benson, W. F. (2008). Peer reviewed: disaster preparedness and the chronic disease needs of vulnerable older adults. Preventing chronic disease, 5(1).

American Psychiatric Association (Ed.). (2022). Diagnostic and statistical manual of mental disorders: DSM-5-TR (Fifth edition, text revision). American Psychiatric Association Publishing.

Biernacki W, Bokwa W, Działek J, Padło T (2009) Społecznos´ci lokalne wobec zagrozen _ ´ przyrodniczych i kle¸sk zywiołowych Wydawnictwo Instytut Geografii i Gospodarki Przestrzennej Uniwersytetu _ Jagiellon´skiego, Krako´w

Bishop, A. W. (1955). The use of the slip circle in the stability analysis of slopes. Geotechnique, 5(1), 7-17.

Bradford, R. A., O'Sullivan, J. J., Van der Craats, I. M., Krywkow, J., Rotko, P., Aaltonen, J., ... & Schelfaut, K. (2012). Risk perception–issues for flood management in Europe. Natural hazards and earth system sciences, 12(7), 2299-2309.

Calcaterra, D., de Riso, R. & Santo, A. 2003. Landslide hazard and risk mapping: experiences from Campania, Italy". In L. Picarelli (Editor). Fast Slope Movements, Prediction and Prevention for Risk Mitigation. Patron Editore, Bologna. Vol. 1: 63-70.

Carver C. S. (1997). You want to measure coping but your protocol's too long: consider the brief COPE. *International journal of behavioral medicine*, *4*(1), 92–100. https://doi.org/10.1207/s15327558ijbm0401_6

Cascini, L. C. J. R. J. O., Bonnard, C., Corominas, J., Jibson, R., & Montero-Olarte, J. (2005). Landslide hazard and risk zoning for urban planning and development. In Landslide risk management (pp. 209-246). CRC Press.

Cianconi, P., Betrò, S., & Janiri, L. (2020). The impact of climate change on mental health: a systematic descriptive review. Frontiers in psychiatry, 11, 490206.

Cummings, E. M., Davies, P. T., & Campbell, S. B. (2020). Developmental psychopathology and family process: Theory, research, and clinical implications. Guilford Publications.

Di Blasio, P. (Ed.). (2005). Tra rischio e protezione: la valutazione delle competenze parentali. Unicopli.

Ding, Y., Du, X., Li, Q., Zhang, M., Zhang, Q., Tan, X., & Liu, Q. (2020). Risk perception of coronavirus

Funded by the European Union. Views and opinions expressed are however those of the author(s) only and do not necessarily reflect those of the European Union. Neither the European Union nor the granting authority can be held responsible for them.

disease 2019 (COVID-19) and its related factors among college students in China during quarantine. PloS one, 15(8), e0237626.

Dupuy, H. J. (1984). The psychological general well-being (PGWB) index. Assessment of quality of life in clinical trials of cardiovascular therapies.

EN 1997-1:2004, Eurocode 7: Geotechnical design – Part 1: General rules, CEN European Committee for Standardization (2004).
Fell, R. 1994. Landslide risk assessment and acceptable risk. Canadian Geotechnical Journal, 31: 261-272.

England, P. (1989). A Feminist Critique of Rational Choice Theories: Implications for Sociology. American Sociologist, 20(1), 14-22.

Fell, R., Ho, K. K., Lacasse, S., & Leroi, E. (2005). A framework for landslide risk assessment and management. In Landslide risk management (pp. 13-36). CRC Press.

Fell, R. & Hartford, D. 1997. Landslide risk management. In D. Cruden and R. Fell (editors). Landslide Risk Assessment. A.A. Balkema Publishers: 51-109.

Fellenius, W. 1936. Calculation of the stability of earth dams. In Transactions of the 2nd Congress on Large Dams, Washington, D.C. International Commission on Large Dams (ICOLD), Paris. Vol. 4, pp. 445–462.

Fernandez, A., Black, J., Jones, M., Wilson, L., Salvador-Carulla, L., Astell-Burt, T., & Black, D. (2015). Flooding and mental health: a systematic mapping review. PloS one, 10(4), e0119929.

Geostudio - Stability Modeling with GeoStudio (2024). SLOPE/W and SEEP/W: User's guide.

Han, Z., Wang, H., Du, Q., & Zeng, Y. (2017). Natural hazards preparedness in Taiwan: A comparison between households with and without disabled members. *Health security*, *15*(6), 575-581

Janbu, N. 1954. Application of composite slip surfaces for stability analysis. In Proceedings of the European Conference on Stabil ity of Earth Slopes, Stockholm. Vol. 3, pp. 43–49.

Kabunga, A., Okalo, P., Nalwoga, V., & Apili, B. (2022). Landslide disasters in eastern Uganda: post-traumatic stress disorder and its correlates among survivors in Bududa district. BMC psychology, 10(1), 287. https://doi.org/10.1186/s40359-022-01001-5

Kumar, M. T., Kar, N., Namboodiri, V., Joy, A., Sreeenivasan, D., Kumar, S., & Bortel, T. V. (2023). Post-traumatic stress and depression following a landslide linked to the 2018 floods in Kerala, India: Relevance of screening. Journal of Emergency Management (Weston, Mass.), 21(1), 85–96.

Lechowska, E. (2018). What determines flood risk perception? A review of factors of flood risk perception and relations between its basic elements. Natural Hazards, 94(3), 1341-1366.

Funded by the European Union. Views and opinions expressed are however those of the author(s) only and do not necessarily reflect those of the European Union. Neither the European Union nor the granting authority can be held responsible for them.

Lechowska, E. (2022). Approaches in research on flood risk perception and their importance in flood risk management: A review. Natural Hazards, 111(3), 2343-2378.

Leone, F., Asté, J.P. & Leroi, E. 1996. Vulnerability assessment f elements exposed to mass moving: working towards a better risk perception. In K. Senneset (Ed.), Landslides, Vol. I: 263-269 Balkema, Rotterdam.

Maltais, D., Tremblay, A. J., Labra, O., Fortin, G., Généreux, M., Roy, M., & Lansard, A. L. (2019). Seniors who experienced the Lac-Mégantic train derailment tragedy: what are the consequences on physical and mental health?. Gerontology and Geriatric Medicine, 5, 2333721419846191.

Marincioni, F. (2020). L'emergenza climatica in Italia: dalla percezione del rischio alle strategie di adattamento. *Geographies of the Anthropocene Book Series*.

Medved, S., Imširagić, A. S., Salopek, I., Puljić, D., Handl, H., Kovač, M., ... & Kuzman, M. R. (2022). Case series: managing severe mental illness in disaster situation: the Croatian experience after 2020 earthquake. Frontiers in psychiatry, 12, 795661.

Miller, Andrew C.; Arquilla, Bonnie (2008). Chronic Diseases and Natural Hazards: Impact of Disasters on Diabetic, Renal, and Cardiac Patients. Prehospital and Disaster Medicine, 23(2), 185–194. doi:10.1017/s1049023x00005835

Morgenstern, N.R., and Price, V.E. 1965. The analysis of the stability of general slip surfaces. Géotechnique, 15(1): 79–93.

Parel, J. T., & Balamurugan, G. (2021). Psychological Issues of People Affected with Flood: A Systematic Review. International Journal of Nursing Education, 13(2).

Paek, H. J., & Hove, T. (2024). Mechanisms of climate change media effects: roles of risk perception, negative emotion, and efficacy beliefs. Health Communication, 1-10.

Peek, L. (2008). Children and disasters: Understanding vulnerability, developing capacities, and promoting resilience—An introduction. Children Youth and Environments, 18(1), 1-29.

Prins, A., Bovin, M. J., Smolenski, D. J., Marx, B. P., Kimerling, R., Jenkins-Guarnieri, M. A., ... & Tiet, Q. Q. (2016). The primary care PTSD screen for DSM-5 (PC-PTSD-5): development and evaluation within a veteran primary care
sample. Journal of General Internal Medicine, 31(10), 1206-1211.

Rammstedt, B., & John, O. P. (2007). Measuring personality in one minute or less: A 10-item short version of the Big Five Inventory in English and German. *Journal of Research in Personality, 41*(1), 203–212. https://doi.org/10.1016/j.jrp.2006.02.001

Remondo, J., González, A., Díaz de Terán, J.R., Cendrero, A., Fabbri, A. & Chung, Ch-J. 2003. Validation of landslide susceptibility maps; examples and applications from a case study in Northern Spain. Natural Hazards, 30: 437-449.

Funded by the European Union. Views and opinions expressed are however those of the author(s) only and do not necessarily reflect those of the European Union. Neither the European Union nor the granting authority can be held responsible for them.

Sharpe, I., & Davison, C. M. (2022). A scoping review of climate change, climate-related disasters, and mental disorders among children in low-and middle-income countries. International journal of environmental research and public health, 19(5), 2896.

Siegrist, M., & Árvai, J. (2020). Risk perception: Reflections on 40 years of research. Risk analysis, 40(S1), 2191-
2206.

Smith, W. G. (2008). Does gender influence online survey participation? A record-linkage analysis of university faculty online survey response behavior. Online submission.

Spence, R.J.S., Zuccaro, G., Petrazzuoli, S. & Baxter, P.J. 2004. Resistance of building to pyroclastic flows: analytical and experimental studies and their application to Vesuvius. Natural hazards Review, 5: 48-59.

Spencer, E. 1967. A method of analysis of the stability of embankments assuming parallel interslice forces. Géotechnique, 17(1): 11–26.

Stewart A. E. (2021). Psychometric Properties of the Climate Change Worry Scale. *International journal of environmental research and public health*, *18*(2), 494. https://doi.org/10.3390/ijerph18020494

Vanapalli, S. K., Fredlund, D. G., Pufahl, D. E., & Clifton, A. W. (1996). Model for the prediction of shear strength with respect to soil suction. Canadian geotechnical journal, 33(3), 379-392.

Van Genuchten, M. T. (1980). A closed-form equation for predicting the hydraulic conductivity of unsaturated soils. Soil science society of America journal, 44(5), 892-898.

Wachinger, G., Renn, O., Bianchizza, C., Coates, T., De Marchi, B., Domènech, L., & Pellizzoni, L. (2010). Risk perception and natural hazards. CapHaz-Net WP3 Report.

Walinski, A., Sander, J., Gerlinger, G., Clemens, V., Meyer-Lindenberg, A., & Heinz, A. (2023). The effects of climate change on mental health. Deutsches Ärzteblatt International, 120(8), 117.

Walker, E. R., McGee, R. E., & Druss, B. G. (2015). Mortality in mental disorders and global disease burden implications: a systematic review and meta-analysis. JAMA psychiatry, 72(4), 334-341.

Walker, B., Davies, W., & Wilson, G. (2007). Practice note guidelines for landslide risk management. Aust. Geomech, 42, 64-109.

White, B. P., Breakey, S., Brown, M. J., Smith, J. R., Tarbet, A., Nicholas, P. K., & Ros, A. M. V. (2023). Mental health impacts of climate change among vulnerable populations globally: an integrative review. Annals of global health, 89(1).

World Health Organization. (1998). Wellbeing measures in primary health care/the DepCare

Funded by the European Union. Views and opinions expressed are however those of the author(s) only and do not necessarily reflect those of the European Union. Neither the European Union nor the granting authority can be held responsible for them.

Project: report on a WHO meeting: Stockholm, Sweden, 12–13 February 1998 (No. WHO/EURO: 1998-4234-43993-62027). World Health Organization. Regional Office for Europe.

Zhao, Y., Jiang, Y., Zhang, W., & Zhu, Y. (2023). Relationship between Risk Perception, Emotion, and Coping Behavior during Public Health Emergencies: A Systematic Review and Meta-Analysis. Systems, 11(4), 181. https://doi.org/10.3390/systems11040181

Zimet, G. D., Dahlem, N. W., Zimet, S. G., & Farley, G. K. (1988). The multidimensional scale of perceived social support. Journal of Personality Assessment, 52(1), 30-41.

Funded by the European Union. Views and opinions expressed are however those of the author(s) only and do not necessarily reflect those of the European Union. Neither the European Union nor the granting authority can be held responsible for them.